Evaluating the impact of Mediterranean overflow on the large-scale Atlantic Ocean circulation using neodymium isotopic composition

Mohamed Ayache, Didier Swingedouw, Christophe Colin, Jean-Claude Dutay

Version of Record: https://www.sciencedirect.com/science/article/pii/S0031018221001449
Manuscript_40b89dd7d34f88e8432062742597295a

Evaluating the impact of Mediterranean Overflow on the large-scale Atlantic Ocean circulation using neodymium isotopic composition

Mohamed Ayache[1,a], Didier Swingedouw[1], Christophe Colin[2], and Jean-Claude Dutay[3]

[1]Laboratoire Environnements et Paléoenvironnements Océaniques et Continentaux (EPOC), UMR 5805, Université de Bordeaux, 33615 Pessac, France
[2]Université Paris-Saclay,CNRS, GEOPS, 91405 Orsay, France
[3]Laboratoire des Sciences du Climat et de l'Environnement LSCE/IPSL, CEA-CNRS-UVSQ, Université Paris-Saclay, 91191 Gif-sur-Yvette, France
[a]now at: Mediterranean Institute of Oceanography (MIO) UM110, 13288, Aix Marseille university, Marseille, France

Correspondence: M. Ayache (mohamed.ayache@mio.osupytheas.fr); D. Swingedouw (didier.swingedouw@u-bordeaux.fr); C. Colin (christophe.colin@universite-paris-saclay.fr); J-C. Dutay (jean-claude.dutay@lsce.ipsl.fr)

Abstract. Palaeo-oceanographical archives in the Mediterranean Sea indicate the occurrence of Sapropel depositions, which are characteristic of anoxic bottom conditions and of a stratified sea. The impact of such drastic changes in the thermohaline circulation of the Mediterranean Sea on the large-scale circulations in the North Atlantic basin is not fully understood. Here we evaluate the impact of a direct perturbation of the Mediterranean Sea circulation through different idealised simulations with freshwater release rates of 20, 50, 100, and 200 mSv (1 mSv=$10^3 m^3/s$), using a the IPSL-CM5A-LR global coupled atmosphere-ocean model, with simulations up to 1000 years long. The simulations are compared to available data for the Mediterranean Sea and the North Atlantic. The Neodymium isotopic composition (ε_{Nd}) anomalies in the North Atlantic are clearly dependent on the rate of fresh water release in the Mediterranean Sea, and subsequent modification of Atlantic meridional overturning circulation (AMOC) intensity and subpolar gyre (SPG) extension. Based on comparison with seawater ε_{Nd} records from Rockall Trough, we suggest that a limited release of freshwater around 50 mSv may be more representative of hydrological conditions of the Mediterranean Sea during the Sapropel S1 deposition. Our results indicate that a decrease in Mediterranean overflow was clearly a factor in the intensification of upper AMOC following the Early Holocene period, when a large eastward expansion of the subpolar gyre is simulated. Also, eastward expansion of the subpolar gyre due to freshwater release in the Mediterranean (*e.g.* Sapropel-like events) and its impact on the ε_{Nd} signature highlight the fact that the modification of ocean circulation in the North Atlantic basin might be more complex than a straightforward change in the AMOC, since there may also be a large impact on barotropic circulation. The simulations also produce a significant decrease in the ε_{Nd} values of the Iceland-Scotland Overflow Water (between -3.5 and -1.3 ε_{Nd} unit), which is consistent with changes observed during the S1 event in the reconstructions. Thus the 3-dimensional changes in baroclinic and barotropic circulations of the ocean, as reconstructed in some ε_{Nd} records, are broadly consistent with the sensitivity simulations performed, and might thus be partly related to changes in Mediterranean overflow, which would have contributed to modification of the Atlantic Ocean circulation following a complex 3-dimensional pattern that is detailed in the paper.

1 Introduction

The Mediterranean Sea is an almost landlocked basin located in a transition zone between subtropical high pressure and subpolar low pressure in the atmosphere. The hydrodynamics of this basin are controlled by wind forcing, heat and freshwater fluxes at the surface, North Atlantic water inflow through the Straits of Gibraltar, and the outflow at depth of Mediterranean water (*e.g.,* Bryden and Kinder, 1991; Tsimplis and Bryden, 2000; García-Lafuente et al., 2011; Struglia et al., 2004). A link with the Mediterranean overflow water (MOW), which might impact on the Atlantic Meridional Overturning Circulation (AMOC), has been proposed (Cacho et al., 1999, 2000, 2001; Bigg and Wadley, 2001; Sierro et al., 2005; Voelker et al., 2006; Penaud et al., 2011; Ivanovic et al., 2013; Bahr et al., 2015). In particular, it has been suggested that the variations in the thermohaline circulation of the Mediterranean Sea, and in consequence the intensity of the MOW, could play a significant role in the modulation of the AMOC through the injection of saline Mediterranean waters into the intermediate North Atlantic (Rogerson et al., 2006; Voelker et al., 2006; Khélifi et al., 2009; Swingedouw et al., 2019).

Many palaeo-studies have focused primarily on the rapid climate variability during the last glacial period and have shown solid evidence for a close connection between changes in North Atlantic hydrography and the climate over the Mediterranean region (Cacho et al., 1999, 2001; Moreno et al., 2005; Sierro et al., 2005; Frigola et al., 2008; Fletcher and Sánchez Goñi, 2008). Nevertheless, this link has remained poorly understood for the Holocene period, which witnessed significant changes in the climate of the North Atlantic and Europe including the Mediterranean area, as recorded by several climatic proxy records (*e.g.,* O'Brien et al., 1995; Came et al., 2007; Repschläger et al., 2017). The AMOC is believed to have been relatively weak during the early Holocene, possibly due to remnant ice-sheet melting (McManus et al., 2004; Blaschek and Renssen, 2013; Ayache et al., 2018), which may have led to reduced northward heat transport and extended sea ice cover (Renssen et al., 2010; Roche et al., 2010; Thornalley et al., 2011, 2013). Proxy data have suggested a greater eastward extension of the subpolar gyre (SPG) during the mid-Holocene period (Thornalley et al., 2009; Staines-Urías et al., 2013; Colin et al., 2010, 2019), coeval with a maximum strength of the Iceland-Scotland Overflow Water (ISOW), possibly leading to reinforcement of AMOC (Colin et al., 2019).

The Mediterranean basin is sensitive to rapid climatic changes in the high latitudes of the Northern Hemisphere (Toucanne et al., 2015; Rogerson et al., 2010) and African monsoon variability on orbital timescales (Bahr et al., 2015). The African monsoon was located further north during the early Holocene period leading to the development of vegetation over part of the present-day Sahara Desert (hypothesis of the Green Sahara, *e.g.,* Rohling et al., 2009; Almogi-Labin et al., 2009; Tierney et al., 2017), and potentially resulting in a very large increase of freshwater input from the river Nile and other North African paleo-rivers (*e.g.,* Rossignol-Strick et al., 1982; Rohling et al., 2002). Marine sedimentation in the eastern Mediterranean Sea was characterized in the past by the deposition of organic-rich dark layers, called sapropels (Rossignol-Strick et al., 1992). The youngest sapropel (termed S1) formed between 10.2-6.4 cal kyr BP (Mercone et al., 2000; De Lange et al., 2008) when anoxic conditions prevailed in the deep Mediterranean Sea, with a reduced oxygen supply to the bottom (De Lange et al., 2008). Possible explanations for such events are (i) a very stratified sea possibly related to freshwater discharge from rivers and runoff, mainly from the Nile River toward the Levantine Sea, (ii) an increased abundance of organic matter sinking from surface water induced by an increase of primary productivity, or a combination of processes (i) and (ii) as proposed by: Cramp and O'Sullivan (1999); Rohling et al. (2015); Rohling (1994); Kallel and Labeyrie (1997); Revel et al. (2010); Bianchi et al. (2006); Myers et al. (1998); Rohling (1994); Stratford et al. (2000). Sapropel events associated with the release of freshwater in line with hypothesis (i) may have led to a marked decrease in deep and intermediate water formation feeding the MOW, as has recently been reconstructed in the Gibraltar Strait (Bahr et al., 2015).

Many studies have investigated the impact of a drastic change in the MOW on Atlantic thermohaline circulation. Rahmstorf (1998), using a simple climate model, showed a small decrease in the AMOC when the MOW ceases. Ivanovic et al. (2014), by changing the salinity of the Mediterranean and the MOW using the HadCM3 climate model, found two opposing responses in the AMOC, namely an enhancement of the upper limb (first 500 m) and a reduction of its deeper limb by 4 Sv (1 Sv=10^6 m^3/s). This complex response was related to changes in zonal and vertical density fields in response to the disappearance of the MOW. New et al. (2001), using a relatively high resolution (1/3°) ocean-only model, showed a strong decrease in the Azores current when the MOW was absent. The waters deviated from the North Atlantic drift, through the Azores current, then simply followed their normal pathway, potentially leading to a larger volume of North Atlantic drift, thus increasing the input of subtropical water towards the North Atlantic, and impacting upon deep convection there. In a recent study, Swingedouw et al. (2019), using the IPSL-CM5A-LR model for a number of multi-centennial sensitivity simulations, revealed the complexity of AMOC response to changes in MOW. These authors suggest that interpreting the reconstructed water mass changes from a single depth has to be treated with a degree of caution and that it may be not representative of large-scale AMOC changes or changes in meridional heat transport, which necessitate an understanding of the changes at different depths and spatial locations.

To overcome this difficulty, the use of an independent proxy of changes in the water masses is required. Neodymium (Nd) isotopic composition ($\varepsilon_{\mathrm{Nd}}$) is particularly useful for gaining a better understanding of the potential link between the MOW and large-scale Atlantic circulation and water mass modifications. Indeed, with a residence time of 500-1000 years (Tachikawa et al., 2003; Arsouze et al., 2009; Siddall et al., 2008) and distinct local basin scale sources (Jeandel et al., 2007; Ayache et al., 2016), Nd isotopes are thought to behave as a quasi-conservative water mass tracer with great potential to fingerprint the provenance of water masses. Furthermore, the upper to mid-depth water mass circulations in the North Atlantic are characterized by contrasted Nd isotopic signatures, ranging from -9.4 for Mediterranean Sea Water (MSW) (Greaves et al., 1991; Henry et al., 1994; Tachikawa et al., 2004; Dubois-Dauphin et al., 2017) and about -10 for water originating from the subtropical Atlantic (Lambelet et al., 2016), down to -15 for water masses originating from the Labrador Sea (Lacan and Jeandel, 2004a; Lambelet et al., 2016; Dubois-Dauphin et al., 2017). In the last decade, a growing number of studies have relied on $\varepsilon_{\mathrm{Nd}}$ records to trace the origin of water masses in modern oceanography (Tachikawa et al., 2017; Lacan and Jeandel, 2004c, 2005c; Piepgras and Wasserburg, 1983; Spivack and Wasserburg, 1988; Tachikawa et al., 2004), and to draw conclusions about past ocean circulation changes during the Holocene (*e.g.,* Colin et al., 2010; Crocket et al., 2011; Xie et al., 2012; Montero-Serrano et al., 2011; Copard et al., 2012). This tracer has notably been used to estimate the eastward extension of the SPG in the north-eastern Atlantic (Colin et al., 2010; Montero-Serrano et al., 2011; Copard et al., 2012; Montero-Serrano et al., 2013; Colin et al., 2019; Dubois-Dauphin et al., 2019).

For the Mediterranean Sea, in the context of sapropel events, ε_{Nd} in marine sediments and cold-water corals allow us to assess the origin of the water masses (Scrivner et al., 2004; Revel et al., 2014; Wu et al., 2019; Duhamel et al., 2020). Dubois-Dauphin et al. (2017) measured ε_{Nd} data obtained from cold-water corals to the south of Sardinia during the Sapropel S1 deposition and found a lower ε_{Nd} during S1, suggesting a significant contribution of intermediate waters originating from the western basin that could have replaced the Levantine intermediate water (LIW). Using data from the Levantine Sea and the Strait of Sicily Cornuault et al. (2018), Wu et al. (2019) and Duhamel et al. (2020) found a marked gradient in ε_{Nd} values between the Eastern and the Western Mediterranean basins, with a more radiogenic ε_{Nd} signature in the Eastern basin during Sapropel events than at present, and a decrease in ε_{Nd} values at the Strait of Sicily after the deposition of sapropel S1; this reflects improved water exchange between both basins which would have led to the modern circulation pattern. Using ε_{Nd} data from fish debris and foraminifera Wu et al. (2019) have shown a decoupled circulation between the eastern and western basins during the sapropel S1 event, and a stagnation of seawater below 800 m depth in the eastern basin. In addition, Duhamel et al. (2020) have suggested that radiogenic seawater ε_{Nd} values observed during African Humid Periods (and sapropel events) are associated with an intensification of Nile discharge and an increase in the residence time of deep-water masses in the eastern Mediterranean Sea, which induces an increase in the interaction between deep-water masses and radiogenic sediments along the margin of the eastern Mediterranean Sea. Vadsaria et al. (2019) performed a set of hosing experiments to perturb the Mediterranean Sea thermohaline circulation with an additional freshwater supply from the Nile River, using a high resolution regional coupled model (LMDz4-NEMO-MED8). They confirmed that an increase in Nile River outflow can trigger the shutdown of eastern Mediterranean convection and creates favourable conditions for anoxic events.

Our aim here is to investigate the extent to which the observed temporal variation in ε_{Nd} reflects changes in the thermohaline circulation of the Mediterranean Sea and to assess its impact on North Atlantic circulation. We evaluate changes in the ε_{Nd} of water masses in the Mediterranean Sea in response to different rates of freshwater release into the basin; these releases are not meant to be realistic in terms of their scale, but serve as sensitivity experiments (*cf.* Appendix B, Fig. A1, and Fig. A2 in appendix). This paper explores the impact of drastic changes in Mediterranean thermohaline circulation on the North Atlantic Circulation and provides quantitative evidence for the impact of an intensification of the AMOC and of a greater eastward extension of the SPG on the Nd isotopic distribution in the Atlantic, similar to the situation that prevailed during the mid-Holocene period. For this purpose, we evaluate the simulated ε_{Nd} distribution in a preindustrial simulation from IPSL-CM5A-LR state-of-the-art climate models. Then we compare simulated ε_{Nd} distribution with different strengths of MOW from different freshwater hosings in the Mediterranean, mimicking the possible cause of a sapropel event during the early Holocene period. The specificity of this study is the use of ε_{Nd} simulated both in the Mediterranean Sea and in the North Atlantic basin using the same model this provides a method to better understand the mechanisms that affected the changes in the proxy distribution observed in the past period. This limits the problems related to the treatment of boundary conditions, and the exchange between the North Atlantic and the Mediterranean Sea (*cf.* Section 2.2). Finally, based on these sensitivity experiments we argue that MOW changes may explain some of the adjustments in Atlantic circulation, which could be a key driver of Holocene variability.

2 Methods

2.1 The IPSL-CM5A global ocean-atmosphere coupled model

In this study, we use the IPSL-CM5A global ocean-atmosphere coupled model IPSL-CM5A (Dufresne et al., 2013) in its low-resolution (LR) version as developed for the Coupled Model Inter-comparison Project Phase 5 (CMIP5). The model is composed of the LMDZ5 atmospheric component (Hourdin et al., 2013) with a 96 × 96 × 39 (longitude × latitude × altitude) regular grid, and the NEMOv3.2 oceanic component (Madec and NEMO-Team., 2008) in ORCA2 configuration (non-regular grid) with 182 × 149 points on 31 vertical levels. The NEMO model also include the LIM-2 sea-ice component (Fichefet and Maqueda, 1997), and PISCES module (Aumont and Bopp, 2006) for oceanic biogeochemistry.

It is important for global climate models to include the effects of salty water entering the North Atlantic from the Mediterranean Sea. Likewise, it is crucial for the Mediterranean Sea to replenish its supply of water from the Atlantic to balance the net evaporation occurring over the Mediterranean Sea. This may explain the degree of care taken to correctly represent the Mediterranean basin in the IPSL-CM5A model, despite its relatively coarse horizontal resolution (ORCA2). Indeed, local modifications of the scale factor have been carried out to the code in order to refine the resolution of the Gibraltar Strait so as to make it more realistic (*cf.* Madec and NEMO-Team., 2008). The ORCA2 configuration use a mesh grid of 20 km at the strait of Gibraltar in order to better reproduce the geometry of the strait. For the grid points located where the strait opens into the Atlantic basin the bottom boundary layer value was enhanced by four in order to model MOW with correct characteristics at equilibrium depth (Beckmann and Döscher, 1997). A similar model was used to study deep-water formation in the Gulf of Lion by Madec and Crepon (1991). More recently Swingedouw et al. (2019) investigated the impact of a freshwater release in the Mediterranean Sea on North Atlantic circulation, with a specific focus on the AMOC. They argued that the parameterization of the MOW in the IPSL-CM5 model (used in this study) is a significant improvement as compared to previous studies that analysed the potential impact of the MOW using simpler and coarser ocean models (*e.g.,* Rahmstorf, 1998; Bigg and Wadley, 2001; Chan and Motoi, 2003; Rogerson et al., 2010; Ivanovic et al., 2013).

2.2 Modelling the Nd isotopic composition

The exchange between the continental margins and seawater, hereafter referred to as boundary exchange (BE), represents the main source of Nd at a global scale (Arsouze et al., 2007, 2010; Rempfer et al., 2011). This source represents more than 95 % of the total input, whereas dissolved riverine and dust inputs are probably only significant in the upper 500 m (Arsouze et al., 2010). The decoupled behaviour observed between $\varepsilon_{\mathrm{Nd}}$ and Nd concentration cycles has led to the notion of a "Nd paradox" (Tachikawa et al., 2003; Lacan and Jeandel, 2005a). While $\varepsilon_{\mathrm{Nd}}$ behaves in a quasi-conservative way in the open ocean, leading to its broad use as a water-mass tracer, Nd concentration displays vertical profiles that increase with depth, together with deep-water enrichment along the global thermohaline circulation (Bertram and Elderfield, 1993; Jeandel et al., 1995; Tachikawa et al., 1999, 2003; Lacan and Jeandel, 2001, 2005a). Since, our aim is to tag water masses with distinct isotopic compositions in order to constrain water mass mixing and pathways, as well as thermohaline circulation, we have chosen to simulate only the Nd isotopic composition ($\varepsilon_{\mathrm{Nd}}$), allowing us to run long simulations of thousands of years with a low computational cost. In fact, simulating both the concentration and isotopic distributions of Nd is more complex and require the use a fully prognostic coupled dynamic/biogeochemical model with an explicit representation of all Nd sources (*i.e.* atmospheric dusts, dissolved river fluxes, and margin sediment re-dissolution) and sinks (*i.e.* scavenging); in reality, past river inputs are also difficult to constrain and very limited river data are available (*cf.* section 4.3 that explicitly addresses the limitations of our modeling approach).

The neodymium isotope tracer is implemented in the IPSL-CM5-LR model, following the protocol developed for the global scale by Arsouze et al. (2007) with a global ocean circulation model (OPA-ORCA2). This simplified modelling approach has already been used in several high computational cost modelling studies such as high resolution regional simulation of the North Atlantic basin (Arsouze et al., 2010) and Mediterranean basin (Ayache et al., 2016; Vadsaria et al., 2019) or long simulation in paleoclimatic studies for investigating the variability of AMOC during the Last Glacial Maximum (LGM) (Arsouze et al., 2008), or the shoaling of the Central American Seaway during the Miocene (Sepulchre et al., 2014).

The $\varepsilon_{\mathrm{Nd}}$ is implemented in the model as a passive conservative tracer which does not affect ocean circulation. Hence, simulations could be run in off-line mode using the pre-computed transport fields at the monthly time scale from the IPSL-CM5A-LR simulations described in Swingedouw et al. (2019). $\varepsilon_{\mathrm{Nd}}$ is transported in the model using a classical advection-diffusion equation, including the sources and sinks (SMS term, eq1). The rate of change of oceanic Nd isotopic composition is:

$$\frac{\delta \varepsilon_{Nd}}{\delta t} = S(\varepsilon_{Nd}) - U \cdot \nabla \varepsilon_{Nd} + \nabla \cdot (K \nabla \varepsilon_{Nd}), \tag{1}$$

where S(ε_{Nd}) represents the SMS term, U $\cdot \nabla \varepsilon_{Nd}$ is the three-dimensional advection and $\nabla \cdot (K \nabla \varepsilon_{Nd})$ is the lateral and vertical diffusion of ε_{Nd}.

The only SMS term considered in the present study is the boundary Exchange (BE) parameterized by the relaxing equation (2) between water mass entering in contact with any margin towards the value of this particular margin:

$$S(\varepsilon_{Nd}) = 1/\tau(\varepsilon_{Ndmargin} - \varepsilon_{Nd}).mask_{margin}, \tag{2}$$

where τ is the characteristic relaxing time (*i.e.* the characteristic time needed to transfer isotopic properties from the continental margin to the ocean). According to Arsouze et al. (2007), the relaxing time is estimated at 1 year for the global scale. $\varepsilon_{\mathrm{Nd}}$ in equation (2) is the Nd isotopic composition of seawater $\varepsilon_{Ndmargin}$ is the value of the material deposited along the continental margin. Its spatial distribution is estimated using the compilation of Jeandel et al. (2007), and $mask_{margin}$ is the percentage of continental margin within the grid box which represents the proportion of the surface within the grid where the BE process occurs (*i.e.* shelf and slope located below this coastline). This quantity is estimated from ETOPO-2 high-resolution bathymetry following the margin definition used to simulate the iron cycle in the PISCES model (Aumont and Bopp, 2006).

We used dissolved $\varepsilon_{\mathrm{Nd}}$ data compiled by Tachikawa et al. (2017), Lambelet et al. (2016), along with additional recent data from Dubois-Dauphin et al. (2017) to evaluate the ability of the model to simulate the main features of the circulation and mixing of the water masses in the Mediterranean Sea and in the North Atlantic basin.

2.3 Sensitivity experiments

We used five existing climate simulations from Swingedouw et al. (2019) to analyse the impact of a change in the MOW intensity on the Nd isotopic distribution and the general circulation in the North Atlantic basin. A 1000-year control simulation under pre-industrial conditions was first run with no change in the freshwater balance of the Mediterranean Sea (*i.e.* evaporation minus precipitation and runoff). This control simulation starts after thousands of years of spin-up procedure and is stable from the beginning of the simulation (for more details, see Swingedouw et al. 2019).

Following Swingedouw et al. (2019), we have used four different simulations with different hosing rates in the Mediterranean Sea (*i.e.* HosMed2, HosMed1, HosMed05, HosMed02), where freshwater is released all over the surface of the Mediterranean Sea with a constant value of 0.2, 0.1, 0.05, and 0.02 Sv, respectively. The freshwater was added following the free surface scheme (Roullet and Madec, 2000) used in NEMO with a constant rate of release throughout the experiments. These different rates are very large, the lowest one HosMed02 corresponds to a River Nile runoff multiplied by around 7. The HosMed1 represents almost a doubling of present-day freshwater forcing (*e.g.* precipitations and runoff) and is therefore very large. However, HosMed2 experiment should not be regarded as realistic and should be taken as an idealized extreme case simulation performed to evaluate the limit of the system analysed. These idealised simulations are principally aimed at analysing the impact of a change in the freshwater balance (*e.g.* Sapropel-like events) on the Nd isotopic composition and on larger-scale circulation, especially in the North Atlantic. A more detailed evaluation of those different rates of hosing is provided in Swingedouw et al. (2019). From these climate simulations, we ran off-line tracer simulations, which were initialized with a uniform isotopic composition of $\varepsilon_{\mathrm{Nd}}$= -7, following the protocol presented in section 2.2.

3 Results

3.1 Validating the control simulation in the Mediterranean Sea and the North Atlantic basin

We have evaluated the control simulation against *in situ* observations made in the Mediterranean Sea (Fig.1), and in the North Atlantic basin (Fig. 2). Figure 1a shows the $\varepsilon_{\mathrm{Nd}}$ distribution over the whole water column in the Mediterranean Sea along a longitudinal transect for both the eastern and western basins. The $\varepsilon_{\mathrm{Nd}}$ horizontal distributions for the surface waters (0-50 m), the intermediate waters (50-750 m) and the deep waters (750-3000 m) are presented in Fig. 1b, 1c, and 1d respectively, together with *in situ* observations from Tachikawa et al. (2004), Vance et al. (2004), and Henry et al. (1994). Figures 1 include also a comparison of average vertical profiles of Nd isotopic signature from control run against in-situ data in the whole Mediterranean Sea. The model results are extracted for the last 100 years of the control simulation.

The surface waters originating from the Atlantic Ocean (Atlantic Waters, AW) are characterized by the most negative signature (value around -9) and are transported all over the Mediterranean Sea, allowing them to be clearly identified; this corresponds well to published *in situ* data from Tachikawa et al. (2004) and Dubois-Dauphin et al. (2017) (Fig.1b). The model simulates a pronounced $\varepsilon_{\mathrm{Nd}}$ east-west gradient in $\varepsilon_{\mathrm{Nd}}$ values, which characterizes the Mediterranean waters (Fig.1), but which is slightly underestimated in the model as compared to *in situ* data.

The values simulated in the Western basin (WMed) and Eastern Levantine basin are consistent with the observations made by Tachikawa et al. (2004). Below a depth of 50 m (Fig. 1c), Levantine Intermediate Water mass (LIW) exhibits higher mean $\varepsilon_{\mathrm{Nd}}$ values of $\sim$ -8, similar to the value of -8.9, -8.7 reported by Tachikawa et al. (2004). The Nd isotopic composition of LIW has been shown to evolve along its westward flow from the formation region in the Levantine Basin ($\varepsilon_{\mathrm{Nd}}$ -4; Tachikawa et al. 2004) through mixing with water masses lying above and below it (Henry et al., 1994). The model captures the general features of the vertical profiles of Nd isotopic signatures in the Mediterranean Sea, although a difference of almost 2 ϵNd units can be found in some places, where the model underestimates *in situ* data from surface and intermediate water-mass, and on the opposite overestimate the ϵNd in the deep water (Fig. 1). The LIW is well identified by its radiogenic signature. LIW is produced in the Levantine sub-basin before passing Crete at 28° E, where measured $\varepsilon_{\mathrm{Nd}}$ values reach -5 (Fig. 1). The model simulates a similar signature (around -5.5) but at relatively deeper levels compared to *in situ* observations (Fig. 1a). A similar bias was simulated by Ayache et al. (2016) and by Vadsaria et al. (2019) even when using high resolution regional models (1/12°, and 1/8° of horizontal resolution respectively). This evaluation shows that despite its low resolution, the model produces a qualitatively correct distribution of the $\varepsilon_{\mathrm{Nd}}$ of the water masses in the semi-enclosed Mediterranean basin (Fig. 1).

We have also evaluated the $\varepsilon_{\mathrm{Nd}}$ distribution in the North Atlantic basin in the control simulation. Figure 2a displays the horizontal distribution of $\varepsilon_{\mathrm{Nd}}$ at intermediate level (750 m depth), and in two vertical sections along the north to equatorial western Atlantic basin (Fig. 2b) and along a latitudinal transect in the western European margin (2c). Figure 2a shows a strong North-South basin scale $\varepsilon_{\mathrm{Nd}}$ contrast, with less radiogenic $\varepsilon_{\mathrm{Nd}}$ values for water masses derived from the Labrador Sea Water (LSW): $\varepsilon_{\mathrm{Nd}}$ -13 to -14.5; North East Atlantic Deep-Water (NEADW): $\varepsilon_{\mathrm{Nd}}$ -12.5 to -13, and North Atlantic Deep-Water (NADW) with $\varepsilon_{\mathrm{Nd}}$ -12.5 to -13 which is similar to observation from Dubois-Dauphin et al. (2017); Lambelet et al. (2016); Lacan and Jeandel (2004b, 2005b) and from Piepgras and Wasserburg (1987). Conversely, $\varepsilon_{\mathrm{Nd}}$ values of water masses from the subtropical gyre (STG; $\varepsilon_{\mathrm{Nd}}$ = -10 to -12) and southern sourced waters, such as Antarctic Bottom Water (AABW) and the Antarctic Intermediate Water (AAIW) ($\varepsilon_{\mathrm{Nd}}$ between -7 and -9 in the Southern Ocean), are characterized by more radiogenic values (Jeandel, 1993; Copard et al., 2011; Stichel et al., 2012). The model correctly simulates the pronounced North-South gradient in $\varepsilon_{\mathrm{Nd}}$ that characterizes surface and intermediate waters in the Atlantic basin (Fig. 2), but overestimate the observed values in the subtropical region. Therefore, the very radiogenic $\varepsilon_{\mathrm{Nd}}$ from *in situ* data located around 30-35°N (Fig. 2b) has been interpreted as a local influence of volcanic material input (*cf.* Tachikawa et al. 2017 for more details).

In the Gulf of Cadiz, the Mediterranean Sea Water (MSW) displays $\varepsilon_{\mathrm{Nd}}$ values that range from -9.5 to -10.1 in close agreement with data from Dubois-Dauphin et al. (2017), in the deep water the $\varepsilon_{\mathrm{Nd}}$ values decrease from -10.2 to -11, which corresponds to ENADW (Fig. 2c). At Rockall Trough, the most unradiogenic $\varepsilon_{\mathrm{Nd}}$ values (-14.0 $\pm$ 0.2 to -14.8 $\pm$ 0.5) correspond to the LSW between a depth of 18000 and 2500 m, thus pointing to a strong influence from water originating in the Labrador Sea (Fig. 2c). However, the model significantly overestimates the $\varepsilon_{\mathrm{Nd}}$ values observed in the surface and intermediate waters in this area (Fig. 2c). This bias will possibly be corrected once the dust and river inputs are included in the model (*e.g.,* Arsouze et al. 2009; Ayache 2016). Nevertheless, we prefer not to use this flux in the present study in order to keep things simple and only evaluate the impact of boundary exchange, notably because estimate of past atmospheric fluxes are hardly available. This shortfall might also be related to the deep convection bias in the physical model, whereby the Labrador Sea convection is shifted to the east (Escudier et al., 2013). In the western part the Nd isotopic composition of AAIW is the result of mixing between radiogenic Pacific water (ε_{Nd} = -4) and unradiogenic Atlantic water (ε_{Nd} = -13.5) in the Southern Ocean, which leads to present-day ε_{Nd} values for AAIW of between -7 and -9 (Jeandel, 1993; Stichel et al., 2012). The AABW is well simulated by the model at a depth of 4000 m where it is characterized by intermediate ε_{Nd} values ($\sim$ -10, Fig. 2b).

In conclusion, this cross-comparison with observations shows that, even though its low resolution limits its ability to resolve mesoscale and convective processes, overall this model simulates the main characteristics of the global ε_{Nd} in the Mediterranean Sea and the North Atlantic basin and associated main water mass signatures. It allows us to gain interesting insights regarding the impact of a perturbation of the Mediterranean outflow. Nevertheless, unavoidable caveats remain, which will be discussed at the end of the paper.

3.2 Spatial cross-correlation between ε_{Nd} and North Atlantic circulation (AMOC, SPG)

To further investigate the relationship between the Nd isotopic composition in the North Atlantic (as a quasi-conservative tracer) and the changes of the North Atlantic ocean circulations (*e.g.,* AMOC and SPG) on a multi-centennial time scale, we have used point correlation maps, which are useful for visualising spatial teleconnections between ε_{Nd} signature and changes in oceanic circulation. Figure 3 shows the spatial variability of correlation between the ε_{Nd} and a subpolar gyre index (defined as the maximum of the absolute value of the barotropic stream function over the subpolar region) from the control simulation. Significant negative correlations are mainly found in the surface and intermediate waters near Iceland (Fig. 3a and Fig. 3b), and positive correlations are located in the southern part of the Labrador Sea (Fig. 3). The same analyses are made between the ε_{Nd} with AMOC index (calculated as the maximum of the annual mean overturning stream function in the Atlantic at 48°N from 500 m to the bottom of the ocean). Again, significant correlations are mainly found in the Labrador Sea and near Iceland (Fig. 4).

All correlation maps show negative correlations in the Labrador Sea for the surface and intermediate waters (Fig. 3 and Fig. 4), indicating that a strong AMOC import more subpolar waters which are tagged by the lowest ε_{Nd} signature in the north Atlantic basin (*cf.* Fig. 2a). The positive correlations represent more radiogenic waters imported from a southern source water (*i.e* sub-tropical water). Indeed, high positive correlation between ε_{Nd} and SPG is simulated over the whole water column to the south of Greenland (at about longitude 50°W and latitude 50°N). This could be associated with deep convection in this area mixing water imported from sub-tropical region (*i.e.* with more radiogenic isotopic signature) from the surface almost to the bottom (in the model), thereby producing a vertically homogenized water column (Fig. 3). Thus, this correlation analysis shows that the model exhibits potential linkages between ε_{Nd} isotopic distribution and large-scale circulation in the Atlantic basin.

3.3 Hosing experiment

3.3.1 Impact of variations in MOW on Nd isotopic signature in the North Atlantic

We have evaluated and discussed the impact of our hosing experiments and the simulated reduced circulation on the $\varepsilon_{\mathrm{Nd}}$ distribution in the Mediterranean Sea (shown in Appendix B section). The impact of the decrease in the MOW at the Straits of Gibraltar on the $\varepsilon_{\mathrm{Nd}}$ in the North Atlantic Ocean is shown in Figure 5. Under pre-industrial condition (Fig. 5a), we can identify the MOW with its radiogenic signature ($\varepsilon_{\mathrm{Nd}}$ = $\sim$ -8.4) at around 1000m depth, while AW is enters at the surface in the Mediterranean Sea with a less radiogenic signature ($\varepsilon_{\mathrm{Nd}}$ = $\sim$ -10 *cf.* Fig. A1 and Fig. A2 in appendix). In most of the hosing simulations, the changes in MOW can be traced through a decrease in $\varepsilon_{\mathrm{Nd}}$ at 1000 m, of 2 $\varepsilon_{\mathrm{Nd}}$ units in HosMed2 and almost 1 $\varepsilon_{\mathrm{Nd}}$ unit in HosMed1 (Fig. 5b, 5c and 5d). HosMed02 shows lower isotopic signature changes but with a similar pattern as the other experiments (Fig. 5e). The longitude-depth section at around 36°N shows an important decrease of $\varepsilon_{\mathrm{Nd}}$ value in the surface water (down to a depth of 1000 m) in the hosing experiments, while deep water exhibits more radiogenic values especially in HosMed2 and HosMed1, indicating a higher contribution of radiogenic waters exported from the Southern Ocean (*i.e.* from the AAIW), and less input from the northern basin (*i.e.* from the Labrador Sea).

The $\varepsilon_{\mathrm{Nd}}$ anomaly across North Atlantic surface water (first 100 m of depth) is shown in Figure 6. We have focused on the first and last century from our experiments to evaluate the relatively rapid adjustment of the Atlantic circulation, and the longer one, which could be key for reconstructed long-term Holocene variability (Swingedouw et al., 2019). In figure 6b we notice a clear drop in $\varepsilon_{\mathrm{Nd}}$ values over the whole North Atlantic basin exceeding 2 $\varepsilon_{\mathrm{Nd}}$ units for the last 100 years (on average) in HosMed2 simulation (Fig. 6b). This drop increases with the rate of freshwater release (*i.e.* maximum in HosMed2 and HosMed1 experiments, and very small in HosMed05 and HosMed02). To clarify this $\varepsilon_{\mathrm{Nd}}$ anomaly in the North Atlantic, we have analysed changes in the upper ocean current (first 100 m); these are also represented in Fig. 6. In the first century, all simulations exhibit an increase in the northward velocity west of the Rockall Trough, associated with an increase in the North Atlantic drift and a decrease in the Azores Current; this is also clear from barotropic stream function representations (Fig. 7). The reduction in the Azores Current can be related to the decrease of MOW as shown in (Jia, 2000) using ocean-only models and in Swingedouw et al. (2019) in these simulations. However as shown by Swingedouw et al. (2019) the Azores Current is weak in the IPSL-CM5 model, possibly due to the coarse horizontal resolution of the ocean model, which is not fine enough to resolve sufficiently this narrow current (see Swingedouw et al. 2019, for more detail on the dynamical response in these simulations).

The $\varepsilon_{\mathrm{Nd}}$ anomaly in the North Atlantic basin at 750 m depth (*i.e.* depth of the paleo-records at Rockall Trough) is shown in Figure 7. The SPG exhibits a less radiogenic $\varepsilon_{\mathrm{Nd}}$ in HoMeds2, HosMed1 and HosMed05, but less intense in HosMed02 relative to the control simulation, the $\varepsilon_{\mathrm{Nd}}$ values decrease, suggesting a change in the Subpolar Mode Waters (SPMW), which have an $\varepsilon_{\mathrm{Nd}}$ value of around $\sim$-14.5 (Dubois-Dauphin et al., 2017). This may result from a greater eastward extension of the mid-depth subpolar gyre or a reduction in MSW formation, probably linked to a variation in deep Mediterranean water production.

Figure. 8 shows the vertical profile of $\varepsilon_{\mathrm{Nd}}$ anomalies as the difference between the control simulation and hosing experiments in order to quantify the impact of our hosing experiments on the $\varepsilon_{\mathrm{Nd}}$ of the Iceland-Scotland Overflow Water (ISOW) identified between 2000 and 2600 m depth south of Iceland (Harvey and Theodorou, 1986) and the North Eastern Atlantic Deep Water (NEADW) between 2000 and 3000 m (Van Aken and de Jong, 2012). The eastward extension of the mid-SPG may lead to an important decrease in the ε_{Nd} of ISOW (between -3.5 in HosMed2 and -1.3 in HosMed02, see Fig. 7c). In contrast, the NEADW signature increases the ε_{Nd} by almost +2 unit in HosMed2, +1.3 in HosMed1, +0.9 in HosMed05 and by +0.5 in HosMed02 relative to the control simulation (Fig. 7b). Consequently, the ε_{Nd} of ISOW and ENADW at 25°W can be linked to the mid-SPG dynamic, where an eastward expansion (westward contraction) of the mid-SPG induces a decrease (increase) of Nd isotopic signatures for ISOW (ENADW). This increase in ENADW production might be related to the increase in Sea Surface Salinity (SSS) found in HosMed05 simulation for instance, due to the increase of North Atlantic Current (NAC) export (*cf.* Swingedouw et al. 2019). This increases the deep water production and density in the Nordic Seas could explain the signature of ε_{Nd} found in Fig.8. Conversely, this slight modification of deep water characteristic toward denser waters might have weakened the ISOW signature.

Within the Rockall Trough a present-day water depth profile of ε_{Nd} show an important variation of ε_{Nd} between surface and deep-water (Fig. 9) (Colin et al., 2010; Dubois-Dauphin et al., 2017; Colin et al., 2019). The most unradiogenic ε_{Nd} values of around -14.0 correspond to the upper (300 m of water). Down between 11000 and 1600 m depth the water column exhibits a narrow range of ε_{Nd} values, from -13 to -13.8 which correspond to SPMW and LSW signature (Dubois-Dauphin et al., 2017). Below 1750 m, the seawater becomes more radiogenic ($\sim$ -12.7) in agreement with a relative higher percentage of ISOW at the Rockall Trough. The control simulation is mainly in agreement with the present-day vertical profile of ε_{Nd} at Rockall Trough especially for surface and intermediate water. However, for the deep water, the model failed to reproduce the radiogenic signature of ISOW at Rockall Trough. This shortcoming might be due the low vertical resolution of the model and the poor resolution of boundary currents and overflows notably due to the coarse horizontal resolution of the ocean model, which is not fine enough to sufficiently resolve ISOW outflow (Swingedouw et al., 2019). The hosing experiments (Fig. 9c) show a pronounced decrease of ε_{Nd} at intermediate levels. The most unradiogenic ε_{Nd} values (up to -16.2, Fig. 9c) are simulated with HosMed2 and HosMed1 between 1500 and 1800 m depth which is indicative of the presence of LSW (New and Smythe-Wright, 2001; Lacan and Jeandel, 2004a).

Finally, figure 10 shows a comparison between model results and a compilation of marine sediments cores from Colin et al. (2019); Roberts and Piotrowski (2015), within the Rockall Trough during the Holocene period. The ε_{Nd} records display significant variations over the Holocene (Fig. 10b, and Fig. A3 in appendix), with more radiogenic values during the late Holocene as compared to the early Holocene. This shift of ε_{Nd} (around 6 BP, *cf.* Fig. 10b and Fig. A3 in appendix) towards more radiogenic values are clearly identified in almost all the cores presented in Fig. 10 b. Indeed, a similar shift is simulated by the model when comparing control simulation (*i.e.* representing the present-day situation) and the hosing experiments (*i.e.* representing the Early Holocene situation) ranging from -13 in the control run to -16.2 in HosMed2 (Fig. 10b). The vertical profile of ε_{Nd} in Fig. 10c shows the change in ε_{Nd} during the early Holocene over the whole water column at Rockall Trough (Fig. 10c). The peak of ε_{Nd} change is marked for the intermediates water up to -16.4 at 1200 m depth. Figure 10d shows the ε_{Nd} change at 750 m depth in the Rockall Trough versus freshwater flux to the Mediterranean Sea in the model compared to data from Colin et al., (2010, 2019) and Crocket et al. (2011). The first experiment (HosMed02) seems to generate a weak change in ε_{Nd} (only 0.4 ε_{Nd} units), the two other experiments (HosMed05 and HosMed1) generate a more realistic change in ε_{Nd} comparable to *in situ* data (from 0.8 ε_{Nd} in HosMed05 to 1.3 ε_{Nd} in HosMed1, *cf.* Fig. 8). The last experiment (HosMed2) generates a too large change in Nd isotopic composition compared to in situ data.

4 Discussion

The different experiments using the IPSL-CM5A-LR model have allowed us to evaluate the impact of a freshening of the Mediterranean Sea on the Nd isotopic signatures in the North Atlantic basin; they have revealed a range of very different possible decreases of MOW, from a total collapse (HosMed2) to a slight reduction of the MOW (HosMed02). By integrating off-line tracer simulations of ε_{Nd}, the simulations have allowed us to examine the potential impact of a Sapropel-like event on the ε_{Nd} in the North Atlantic basin and, *in fine*, on the AMOC. Nevertheless, our study does not aim to properly simulate the sapropel S1 event from its onset to the deposit, since our model setup did not consider major forcing needed for the development of an anoxic environment and for the deposition of S1 (*e.g.* sea level rise, climate). The simulations should only be considered as sensitivity experiments that help us to better understand processes at play in response to large releases of freshwater in the Mediterranean Sea. Furthermore a proper simulation of the Mediterranean Sea circulation would require a higher resolution model (*e.g.* 1/8° , 1/12°) that is far beyond the scope of this global-scale modelling study.

4.1 MOW impact on Rockall Trough seawater ϵNd during the Early Holocene period

The ε_{Nd} record in the Rockall Trough shown in figure 10 displays significant variations of about 2.7 ε_{Nd} units between 7 and 5 ka marked by a shift towards more radiogenic isotopic signature, whose timing coevals with the end of the sapropel S1 event (between 10.2-6.4 cal kyr BP). The MOW decrease simulated in our hosing experiments can be clearly invoked as having had an important impact on the Nd isotopic composition around the NE Atlantic basin as shown in figures 8, 9, 10. The maximum of ε_{Nd} shift is well identified in intermediate water (Fig. 10c), where subsurface to intermediate water masses are marked by more radiogenic isotopic signature. The presence of the radiogenic MSW at greater water depth (around 950m) in the Eastern Rockall Trough has been shown to respond to the dynamics of the mid-SPG, such that mid-SPG contraction induces northward penetration of MSW along the western European margin (Lozier and Stewart, 2008). Hence, by vertical mixing and re-circulation (Penny Holliday et al., 2000; Lavender et al., 2005) the MSW could also induce a more radiogenic ϵNd signature to intermediate water masses of the Rockall Trough.

Based on the comparison between the model output and ε_{Nd} simulation with Rockall Trough records, we suggest that HosMed05 may be more representative of hydrological conditions of the Mediterranean Sea and NE Atlantic basin during the deposition of sapropel S1, and the HosMed1 may provide a upper limit. Furthermore, different paleo-proxies collected from the Gulf of Cadiz in the Gibraltar Strait seem to indicate that the MOW was weakened but not suppressed during Sapropel events (*e.g.,* Bahr et al., 2015). Swingedouw et al. (2019) assessed that the amount of freshwater added in HosMed2 (*i.e.* 0.2 Sv) and in HosMed1 (*i.e.* 0.1 Sv) may overestimate the freshwater input during the sapropel event, and the potential fluxes are likely to be lower than 0.1 Sv in total, even during periods of peak Fennoscandian ice sheet melting. To validate and better quantify our hypothesis regarding the impact of the freshening the Mediterranean Sea on ε_{Nd} distribution and ocean dynamics in the North Atlantic, transient simulations over large periods of the Holocene will be necessary.

4.2 The reorganization of mid-depth circulation in the North Atlantic during the Holocene

A major hydro-dynamical re-organization occurred in the North Atlantic during the mid-Holocene period, with a maximum strength of the Iceland-Scotland Overflow Water (ISOW), which might be indicative of an increase in the AMOC. The onset of modern Labrador Sea Water formation is believed to have started from around 7 ka, and was followed by a decrease of the ISOW strength and a contraction of the mid-SPG (*e.g.* Hillaire-Marcel et al., 2001; Colin et al., 2019). An intensification of the upper AMOC cell has also been suggested the Early Holocene period, as demonstrated by sortable silt proxy from Thornalley et al. (2013) and by Ayache et al. (2018) using 22 cores of annual Sea Surface Temperature (SST) compiled in the North Atlantic and covering the Holocene (HAMOC database). Based on the results from the hosing experiments, the freshwater release in the Mediterranean Sea during S1 might have contributed to such a change, with key impacts on radiogenic Nd isotopic signature as illustrated in figures 8, 9, 10.

Also, the intense SPG circulation during the Early to mid-Holocene period may have entrained more unradiogenic ε_{Nd} from the surface water of the Labrador Sea at intermediate depth (between 700 and 1000 m), which is marked by boundary exchange (Lambelet et al., 2016; Colin et al., 2019). This strong early Holocene eastward extension of the SPG circulation would have brought a greater volume of unradiogenic seawater into contact with the ISOW south of Iceland. Thus, it is possible that such an intensification of SPG circulation could have also increased the Nd input from the boundary exchange (Colin et al., 2019). Such an increase of lithogenic Nd input could significantly modify the ε_{Nd} of water masses in the North Atlantic basin. As illustrated in figure 8, the LSW (characterized by unradiogenic ε_{Nd}) are entrained and mixed with the ISOW (characterized by more radiogenic ε_{Nd}). This entrainment of surrounding waters could largely modify the ISOW signature (up to 2.5 ε_{Nd} unit in MedHos1). This increased flow of surface and sub-surface waters, characterized by unradiogenic Nd isotopic signatures, in the Iceland basin may then have been entrained by an intense ISOW during the early to mid-Holocene (Thornalley et al., 2013). Otherwise Howe et al. (2016) suggested that increased detrital input from the Laurentide Ice Sheet in the Early Holocene (Kurzweil et al., 2010) would have induced a modification of the ε_{Nd} of deep-water masses of the North Atlantic. However, Colin et al. (2019) argued that the variation of Nd isotopic composition of the water in the east Atlantic basin during the mid-Holocene cannot be explained solely by the Laurentide Ice Sheet, because melting of the Laurentide Ice Sheet was greater in the early Holocene than during the mid-Holocene, and also similar millennial variation in ε_{Nd} (up to 2.5 ε_{Nd} units) have been observed during the late Holocene period, while the final demise of the Laurentide Ice Sheet occurred earlier (around 6.8 ka, Carlson et al. 2008). Thus, this would have contributed, along with the Nd lithogenic input from detrital material from the Laurentide Ice Sheet (Howe et al., 2016), to the unradiogenic Nd signature observed for the NADW in the Early Holocene in several deep sites of the North Atlantic (Roberts et al., 2010; Böhm et al., 2015; Howe et al., 2016; Lippold et al., 2016). Our simulations indicate that a significant part of the ε_{Nd} signal could be attributed to changes in large-scale circulation associated with MOW outflow reduction.

An important question that remains is, how much did a potential decrease in MOW over the Early Holocene contribute to the observed shift in the ε_{Nd} of SPG? In the North Atlantic basin, as shown by our hosing experiments over the Mediterranean Sea, the decrease of MOW led to an important decrease of ε_{Nd} in the North Atlantic basin as a consequence of less MSW (radiogenic signature) and more LSW (unradiogenic water), similar to the situation during the Early Holocene (*i.e.* an AMOC strengthening) as shown in many studies using different types of records (*e.g.* Ayache et al., 2018; Thornalley et al., 2013). However, additional palaeorecords of ε_{Nd} from the North Atlantic and Mediterranean Sea may help to better constrain the role of MSW changes during the Holocene and therefore the potential impact on ε_{Nd} shift during the mid-Holocene.

4.3 Evaluation and main limitation of ε_{Nd} modelling approach

A key aspect of our analyses concerns the validation of the control run, in simulating the present-day observed distribution of ε_{Nd} both in the Mediterranean Sea and in the North Atlantic basin against *in situ* data. Despite the low resolution of the IPSL-CM5A-LR in the Mediterranean Sea, the model produced reasonable east-west ε_{Nd} gradients for the intermediate and deep-water masses of the Mediterranean Sea (Tachikawa et al., 2004). For the North Atlantic basin, the signature for the main water masses (NADW, AAIW, and AABW) are simulated with realistic ε_{Nd} values. The inter-gyre gradient between SPG (source of less radiogenic water) and STG (source of more radiogenic water) is correctly simulated by the model (*cf.* subsection 3.1). Since we only use boundary exchange as a source of ε_{Nd}, this reinforces the idea of this process as being the major source in the Nd oceanic cycle, even at regional scale and in a semi-enclosed basin such as the Mediterranean basin, in agreement with what has been previously evaluated for the global ocean (Arsouze et al., 2007; Sepulchre et al., 2014; Rempfer et al., 2011), the Atlantic basin (Arsouze et al., 2010), and in the Mediterranean Sea (Ayache et al., 2016). Although the processes leading to boundary exchange are still not fully understood (Jeandel and Oelkers, 2015), the simulated ε_{Nd} is very useful for assessing changes in oceanic circulation during the sapropel event, as also shown in Vadsaria et al. (2019).

It is clear that simulating both the concentration and isotopic distributions of Nd could allow a better evaluation of the lithogenic Nd inputs to the sub-polar water and its impact on the ε_{Nd} in the North Atlantic (*cf.* Section 2.2), and taking into account dust and river input could improve the simulation of Nd distribution. However, past dust input is also difficult to constrain: while flux is sporadic and hard to characterize, establishing the fraction dissolved at the air–sea interface is also challenging, and there is very little available data for rivers. This first idealized modelling approach has demonstrated the advantages of combining observations with numerical simulations, and is a motivation to continue this effort with more sophisticated models. A more substantial data-set available for the Holocene period might be also useful to allow a more in-depth model-data comparison.

For further improving of our modelling approach, including more processes might be required, for instance through the use of a fully prognostic coupled dynamical/biogeochemical model with an explicit representation of all Nd sources (*i.e.* atmospheric dusts, dissolved river fluxes, and margin sediment re-dissolution) and sinks (*i.e.* scavenging) which however remains very costly with such resolution for the Holocene period. Another limitation of the present study concerns the ocean resolution in the Mediterranean Sea, which does not properly resolve meso-scale dynamics which play a key role in the dynamics of both the MOW and the Azores Current in the Atlantic basin (*e.g.* New et al., 2001). It should also be noted that a full understanding of the S1 event necessitates a representation of the whole hydrological cycle of the Early Holocene climate over the Mediterranean basin. Currently, there is no available transient simulation of the Holocene with the IPSL model, (very costly at such a resolution). The use of transient simulation could offer an interesting test-bed to better understand the impact of Sapropel events on large-scale circulation in the North Atlantic over the Holocene and the onset of the modern circulation. Finally, we argue that a full monitoring of the MOW would be useful to estimate and predict potential impacts of MOW variations on the large-scale ocean at long-term time scales.

5 Conclusions

The present study provides new insights concerning the potential impact of enhanced freshwater input into the Mediterranean Sea on the Nd isotopic composition in both the Mediterranean Sea and the North Atlantic basin, and, *in fine*, on the large-scale ocean circulation, as it might have been the case during Sapropel S1 event in the early Holocene. It is based on a set of five IPSL-CM5A-LR long simulations (up to 1000 years). Even though the convective processes are poorly resolved in the IPSL-CM5A-LR model, the Nd isotopic signature of the main water masses in the Mediterranean (*i.e.* reasonable east-west gradients of $\varepsilon_{\mathrm{Nd}}$) and in the north Atlantic basins (the main water masses: NADW, AAIW, AABW) are simulated and allow an evaluation of the impact of a direct perturbation of the Mediterranean Sea circulation (*i.e.* the sapropel-like event).

The hosing experiments in the Mediterranean Sea generally reproduces less radiogenic water masses in the western Mediterranean basin, which is a result of reduced exchange with the eastern basin as indicated by observations. $\varepsilon_{\mathrm{Nd}}$ anomalies are more radiogenic in the eastern Mediterranean basin consequence of the sluggish circulation simulated in hosing experiments. It reproduces stagnation in deep waters that generates an $\varepsilon_{\mathrm{Nd}}$ signature closer to the value of the surrounding margins.

Our different experiments have allowed us to examine the potential impact of a freshwater release in the Mediterranean Sea, leading to a decrease of the MOW, and imprints on the Nd isotopic signatures in the North Atlantic basin with very different possibilities. A freshwater release rate of 0.02 Sv generates a weak change of only 0.4 units in the $\varepsilon_{\mathrm{Nd}}$ at Rockall Trough, while two intermediate experiments (0.05 Sv for HosMed05 and 0.1 Sv for HosMed1) seem to generate change in $\varepsilon_{\mathrm{Nd}}$ more in line with differences between early and late Holocene from *in situ* data (from 0.8 and 1.3 $\varepsilon_{\mathrm{Nd}}$ respectively), which might be possibly representative of the impact of Sapropel S1 event on ocean circulation. The last experiment with a freshwater release rate of 0.2 Sv generate a huge change in $\varepsilon_{\mathrm{Nd}}$ isotopic values. Based on the comparison between the model output and $\varepsilon_{\mathrm{Nd}}$ data, we suggest that HosMed05 may be more representative of hydrological conditions of the Mediterranean Sea during the deposition of Sapropel S1, and that the HosMed1 may provide a very upper limit. To validate and better quantify the impact of a freshening of the Mediterranean Sea on Holocene variability, transient simulations over large periods of the Holocene will be necessary and are planned in future work. The intense SPG circulation (*i.e.* eastward extension of the mid-SPG) during the early to mid-Holocene period may have brought a greater volume of unradiogenic seawater into contact with the ISOW south of Iceland, and would thus have led to an important decrease in $\varepsilon_{\mathrm{Nd}}$ of ISOW (between -3.5 $\varepsilon_{\mathrm{Nd}}$ unit in HosMed2 and -1.3 $\varepsilon_{\mathrm{Nd}}$ unit in HosMed02). Thus, it is possible that such an intensification of SPG circulation, due to a decrease in MOW, could also have increased the lithogenic Nd input from unradiogenic sedimentary margins of the Labrador Sea through the process of Boundary Exchange. Finally, we have demonstrated that the variation in Nd isotopic composition of deep-water masses in the east North Atlantic basins during the mid-Holocene cannot be explained solely by lithogenic Nd input from the Laurentide Ice Sheet but that changes in the intensity of the AMOC and SPG intensity over the course of the Holocene have had a major influence.

Code availability. The model used in this work is IPSL-CM5 Earth System Model platform in its low resolution from (Dufresne et al., 2013). *cf.* https://www.nemo-ocean.eu/.

Data availability. The data associated with the paper are available from the corresponding author upon request. All of the data used in this study were published by their authors as cited in the paper.

Author contributions. This study was co-designed and approved by all co-authors. All co-authors have been involved in the writing and revision of the manuscript.

Acknowledgements. The research leading to this study has received funding from the French National Research Agency HAMOC project under grant ANR-13-BS06-0003. It was also funded by Blue-Action (The European Union's Horizon 2020 research and innovation program, Grant Number: 727852)

References

Almogi-Labin, A., Bar-Matthews, M., Shriki, D., Kolosovsky, E., Paterne, M., Schilman, B., Ayalon, A., Aizenshtat, Z., and Matthews, A.: Climatic variability during the last 90 ka of the southern and northern Levantine Basin as evident from marine records and speleothems, Quaternary Science Reviews, 28, 2882–2896, https://doi.org/10.1016/j.quascirev.2009.07.017, 2009.

Arsouze, T., Dutay, J. C., Lacan, F., and Jeandel, C.: Modeling the neodymium isotopic composition with a global ocean circulation model, Chemical Geology, 239, 165–177, https://doi.org/10.1016/j.chemgeo.2006.12.006, 2007.

Arsouze, T., Dutay, J.-C., Kageyama, M., Lacan, F., Alkama, R., Marti, O., and Jeandel, C.: A modeling sensitivity study of the influence of the Atlantic meridional overturning circulation on neodymium isotopic composition at the Last Glacial Maximum, Climate of the Past, 4, 191–203, https://doi.org/10.5194/cp-4-191-2008, http://www.clim-past.net/4/191/2008/, 2008.

Arsouze, T., Dutay, J.-C., Lacan, F., and Jeandel, C.: Reconstructing the Nd oceanic cycle using a coupled dynamical – biogeochemical model, https://doi.org/10.5194/bgd-6-5549-2009, 2009.

Arsouze, T., Treguier, a. M., Peronne, S., Dutay, J. C., Lacan, F., and Jeandel, C.: Modeling the Nd isotopic composition in the North Atlantic basin using an eddy-permitting model, Ocean Science, 6, 789–797, https://doi.org/10.5194/os-6-789-2010, 2010.

Aumont, O. and Bopp, L.: Globalizing results from ocean in situ iron fertilization studies, Global Biogeochemical Cycles, 20, n/a–n/a, https://doi.org/10.1029/2005GB002591, http://doi.wiley.com/10.1029/2005GB002591, 2006.

Ayache, M.: Modélisation d'éléments traces (T, 3He, Nd, 14C) en mer Méditerranée pour l'étude des cycles biogéochimiques et de la circulation océanique, Ph.D. thesis, Université Paris-Saclay, https://doi.org/NNT : 2016SACLV138, https://tel.archives-ouvertes.fr/tel-01537915, 2016.

Ayache, M., Dutay, J.-C., Arsouze, T., Révillon, S., Beuvier, J., and Jeandel, C.: High-resohlution neodymium characterization along the Mediterranean margins and modelling of ϵNd distribution in the Mediterranean basins, Biogeosciences, 13, 5259–5276, https://doi.org/10.5194/bg-13-5259-2016, http://www.biogeosciences.net/13/5259/2016/, 2016.

Ayache, M., Swingedouw, D., Mary, Y., Eynaud, F., and Colin, C.: Multi-centennial variability of the AMOC over the Holocene: A new reconstruction based on multiple proxy-derived SST records, Global and Planetary Change, 170, 172–189, https://doi.org/10.1016/j.gloplacha.2018.08.016, 2018.

Bahr, A., Kaboth, S., Jiménez-Espejo, F. J., Sierro, F. J., Voelker, A. H., Lourens, L., Röhl, U., Reichart, G. J., Escutia, C., Hernández-Molina, F. J., Pross, J., and Friedrich, O.: Persistent monsoonal forcing of mediterranean outflow water dynamics during the late Pleistocene, Geology, 43, 951–954, https://doi.org/10.1130/G37013.1, 2015.

Beckmann, A. and Döscher, R.: A method for improved representation of dense water spreading over topography in geopotential-coordinate models, Journal of Physical Oceanography, 27, 581–591, https://doi.org/10.1175/1520-0485(1997)027<0581:AMFIRO>2.0.CO;2, 1997.

Bertram, C. J. and Elderfield, H.: The geochemical balance of the rare earth elements and neodymium isotopes in the oceans, Geochimica et Cosmochimica Acta, 57, 1957–1986, https://doi.org/10.1016/0016-7037(93)90087-D, 1993.

Bianchi, D., Zavatarelli, M., Pinardi, N., Capozzi, R., Capotondi, L., Corselli, C., and Masina, S.: Simulations of ecosystem response during the sapropel S1 deposition event, Palaeogeography, Palaeoclimatology, Palaeoecology, 235, 265–287, https://doi.org/10.1016/j.palaeo.2005.09.032, 2006.

Bigg, G. R. and Wadley, M. R.: Millennial-scale variability in the oceans: An ocean modelling view, Journal of Quaternary Science, 16, 309–319, https://doi.org/10.1002/jqs.599, 2001.

Blaschek, M. and Renssen, H.: Climate of the Past The impact of early Holocene Arctic shelf flooding on climate in an atmosphere-ocean-sea-ice model, Clim. Past, 9, 2651–2667, https://doi.org/10.5194/cp-9-2651-2013, www.clim-past.net/9/2651/2013/, 2013.

Böhm, E., Lippold, J., Gutjahr, M., Frank, M., Blaser, P., Antz, B., Fohlmeister, J., Frank, N., Andersen, M. B., and Deininger, M.: Strong and deep Atlantic meridional overturning circulation during the last glacial cycle, Nature, 517, 73–76, https://doi.org/10.1038/nature14059, http://www.nature.com/articles/nature14059, 2015.

Bryden, H. L. and Kinder, T. H.: Steady two-layer exchange through the Strait of Gibraltar, Deep Sea Research Part A. Oceanographic Research Papers, 38, S445–S463, https://doi.org/10.1016/s0198-0149(12)80020-3, 1991.

Cacho, I., Pelejero, C., Grimalt, J. O., Calafat, A., and Canals, M.: C37 alkenone measurements of sea surface temperature in the Gulf of Lions (NW Mediterranean), Organic Geochemistry, 30, 557–566, https://doi.org/10.1016/S0146-6380(99)00038-8, 1999.

Cacho, I., Grimalt, J. O., Sierro, F. J., Shackleton, N., and Canals, M.: Evidence for enhanced Mediterranean thermohaline circulation during rapid climatic coolings, Earth and Planetary Science Letters, 183, 417–429, https://doi.org/10.1016/S0012-821X(00)00296-X, 2000.

Cacho, I., Grimalt, J. O., Canals, M., Sbaffi, L., Shackleton, N. J., Schönfeld, J., and Zahn, R.: Variability of the Western Mediterranean sea surface temperature during the last 25,000 years and its connection with the Northern Hemisphere climatic changes, Paleoceanography, 16, 40–52, https://doi.org/10.1029/2000PA000502, 2001.

Came, R. E., Oppo, D. W., and McManus, J. F.: Amplitude and timing of temperature and salinity variability in the subpolar North Atlantic over the past 10 k.y., Geology, 35, 315–318, https://doi.org/10.1130/G23455A.1, 2007.

Carlson, A. E., LeGrande, A. N., Oppo, D. W., Came, R. E., Schmidt, G. A., Anslow, F. S., Licciardi, J. M., and Obbink, E. A.: Rapid early Holocene deglaciation of the Laurentide ice sheet, Nature Geoscience, 1, 620–624, https://doi.org/10.1038/ngeo285, http://www.nature.com/doifinder/10.1038/ngeo285, 2008.

Chan, W. and Motoi, T.: Effects of stopping the Mediterranean outflow on the southern polar region, Polar Meteorol, Polar Meteorol. Glaciol, 17, 25–35, 2003.

Colin, C., Frank, N., Copard, K., and Douville, E.: Neodymium isotopic composition of deep-sea corals from the NE Atlantic: implications for past hydrological changes during the Holocene, Quaternary Science Reviews, 29, 2509–2517, https://doi.org/10.1016/j.quascirev.2010.05.012, 2010.

Colin, C., Tisnérat-Laborde, N., Mienis, F., Collart, T., Pons-Branchu, E., Dubois-Dauphin, Q., Frank, N., Dapoigny, A., Ayache, M., Swingedouw, D., Dutay, J. C., Eynaud, F., Debret, M., Blamart, D., and Douville, E.: Millennial-scale variations of the Holocene North Atlantic mid-depth gyre inferred from radiocarbon and neodymium isotopes in cold water corals, Quaternary Science Reviews, 211, 93–106, https://doi.org/10.1016/j.quascirev.2019.03.011, 2019.

Copard, K., Colin, C., Frank, N., Jeandel, C., Montero-Serrano, J.-C., Reverdin, G., and Ferron, B.: Nd isotopic composition of water masses and dilution of the Mediterranean outflow along the southwest European margin, Geochemistry, Geophysics, Geosystems, 12, n/a–n/a, https://doi.org/10.1029/2011GC003529, http://doi.wiley.com/10.1029/2011GC003529, 2011.

Copard, K., Colin, C., Henderson, G. M., Scholten, J., Douville, E., Sicre, M. A., and Frank, N.: Late Holocene intermediate water variability in the northeastern Atlantic as recorded by deep-sea corals, Earth and Planetary Science Letters, 313-314, 34–44, https://doi.org/10.1016/j.epsl.2011.09.047, 2012.

Cornuault, M., Tachikawa, K., Vidal, L., Guihou, A., Siani, G., Deschamps, P., Bassinot, F., and Revel, M.: Circulation Changes in the Eastern Mediterranean Sea Over the Past 23,000 Years Inferred From Authigenic Nd Isotopic Ratios, Paleoceanography and Paleoclimatology, 33, 264–280, https://doi.org/10.1002/2017PA003227, 2018.

Cramp, A. and O'Sullivan, G.: Neogene sapropels in the Mediterranean: A review, Marine Geology, 153, 11–28, https://doi.org/10.1016/S0025-3227(98)00092-9, 1999.

Crocket, K. C., Vance, D., Gutjahr, M., Foster, G. L., and Richards, D. A.: Persistent Nordic deep-water overflow to the glacial North Atlantic, Geology, 39, 515–518, https://doi.org/10.1130/G31677.1, 2011.

De Lange, G. J., Thomson, J., Reitz, A., Slomp, C. P., Speranza Principato, M., Erba, E., and Corselli, C.: Synchronous basin-wide formation and redox-controlled preservation of a Mediterranean sapropel, Nature Geoscience, 1, 606–610, https://doi.org/10.1038/ngeo283, 2008.

Dubois-Dauphin, Q., Montagna, P., Siani, G., Douville, E., Wienberg, C., Hebbeln, D., Liu, Z., Kallel, N., Dapoigny, A., Revel, M., Pons-Branchu, E., Taviani, M., and Colin, C.: Hydrological variations of the intermediate water masses of the western Mediterranean Sea during the past 20 ka inferred from neodymium isotopic composition in foraminifera and cold-water corals, Climate of the Past, 13, 17–37, https://doi.org/10.5194/cp-13-17-2017, http://www.clim-past.net/13/17/2017/, 2017.

Dubois-Dauphin, Q., Colin, C., Elliot, M., Dapoigny, A., and Douville, E.: Holocene shifts in sub-surface water circulation of the North-East Atlantic inferred from Nd isotopic composition in cold-water corals, Marine Geology, 410, 135–145, https://doi.org/10.1016/j.margeo.2019.01.004, 2019.

Dufresne, J. L., Foujols, M. A., Denvil, S., Caubel, A., Marti, O., Aumont, O., Balkanski, Y., Bekki, S., Bellenger, H., Benshila, R., Bony, S., Bopp, L., Braconnot, P., Brockmann, P., Cadule, P., Cheruy, F., Codron, F., Cozic, A., Cugnet, D., de Noblet, N., Duvel, J. P., Eth??, C., Fairhead, L., Fichefet, T., Flavoni, S., Friedlingstein, P., Grandpeix, J. Y., Guez, L., Guilyardi, E., Hauglustaine, D., Hourdin, F., Idelkadi, A., Ghattas, J., Joussaume, S., Kageyama, M., Krinner, G., Labetoulle, S., Lahellec, A., Lefebvre, M. P., Lefevre, F., Levy, C., Li, Z. X., Lloyd, J., Lott, F., Madec, G., Mancip, M., Marchand, M., Masson, S., Meurdesoif, Y., Mignot, J., Musat, I., Parouty, S., Polcher, J., Rio, C., Schulz, M., Swingedouw, D., Szopa, S., Talandier, C., Terray, P., Viovy, N., and Vuichard, N.: Climate change projections using the IPSL-CM5 Earth System Model: From CMIP3 to CMIP5, vol. 40, https://doi.org/10.1007/s00382-012-1636-1, 2013.

Duhamel, M., Colin, C., Revel, M., Siani, G., Dapoigny, A., Douville, E., Wu, J., Zhao, Y., Liu, Z., and Montagna, P.: Variations in eastern Mediterranean hydrology during the last climatic cycle as inferred from neodymium isotopes in foraminifera, Quaternary Science Reviews, 237, 106 306, https://doi.org/10.1016/j.quascirev.2020.106306, 2020.

Escudier, R., Mignot, J., and Swingedouw, D.: A 20-year coupled ocean-sea ice-atmosphere variability mode in the North Atlantic in an AOGCM, Climate Dynamics, 40, 619–636, https://doi.org/10.1007/s00382-012-1402-4, 2013.

Fichefet, T. and Maqueda, M. A. M.: Sensitivity of a global sea ice model to the treatment of ice thermodynamics and dynamics, Journal of Geophysical Research: Oceans, 102, 12 609–12 646, https://doi.org/10.1029/97JC00480, http://onlinelibrary.wiley.com/doi/10.1029/97JC00480/abstract, 1997.

Fletcher, W. J. and Sánchez Goñi, M. F.: Orbital- and sub-orbital-scale climate impacts on vegetation of the western Mediterranean basin over the last 48,000 yr, Quaternary Research, 70, 451–464, https://doi.org/10.1016/j.yqres.2008.07.002, 2008.

Frigola, J., Moreno, A., Cacho, I., Canals, M., Sierro, F. J., Flores, J. A., and Grimalt, J. O.: Evidence of abrupt changes in Western Mediterranean Deep Water circulation during the last 50 kyr: A high-resolution marine record from the Balearic Sea, Quaternary International, 181, 88–104, https://doi.org/10.1016/j.quaint.2007.06.016, 2008.

García-Lafuente, J., Sánchez-Román, A., Naranjo, C., and Snchez-Garrido, J. C.: The very first transformation of the Mediterranean outflow in the Strait of Gibraltar, Journal of Geophysical Research: Oceans, 116, https://doi.org/10.1029/2011JC006967, 2011.

Greaves, M. J., Rudnicki, M., and Elderfield, H.: Rare earth elements in the Mediterranean Sea and mixing in the Mediterranean outflow, Earth and Planetary Science Letters, 103, 169–181, https://doi.org/10.1016/0012-821X(91)90158-E, 1991.

Harvey, J. and Theodorou, A.: The circulation of Norwegian Sea overflow water in the eastern North Atlantic, Oceanologica Acta, 9, 393–402, 1986.

Henry, F., Jeandel, C., Dupré, B., and Minster, J.-F.: Particulate and dissolved Nd in the western Mediterranean Sea: Sources, fate and budget, Marine Chemistry, 45, 283–305, https://doi.org/10.1016/0304-4203(94)90075-2, 1994.

Hillaire-Marcel, C., de Vernal, A., Bilodeau, G., and Weaver, A. J.: Absence of deep-water formation in the Labrador Sea during the last interglacial period, Nature, 410, 1073–1077, https://doi.org/10.1038/35074059, http://www.nature.com/doifinder/10.1038/35074059, 2001.

Hourdin, F., Foujols, M.-A., Codron, F., Guemas, V., Dufresne, J.-L., Bony, S., Denvil, S., Guez, L., Lott, F., Ghattas, J., Braconnot, P., Marti, O., Meurdesoif, Y., and Bopp, L.: Impact of the LMDZ atmospheric grid configuration on the climate and sensitivity of the IPSL-CM5A coupled model, Climate Dynamics, 40, 2167–2192, https://doi.org/10.1007/s00382-012-1411-3, http://link.springer.com/10.1007/s00382-012-1411-3, 2013.

Howe, J. N., Piotrowski, A. M., and Rennie, V. C.: Abyssal origin for the early Holocene pulse of unradiogenic neodymium isotopes in Atlantic seawater, Geology, 44, 831–834, https://doi.org/10.1130/G38155.1, 2016.

Ivanovic, R. F., Valdes, P. J., Flecker, R., Gregoire, L. J., and Gutjahr, M.: The parameterisation of Mediterranean-Atlantic water exchange in the Hadley Centre model HadCM3, and its effect on modelled North Atlantic climate, Ocean Modelling, 62, 11–16, https://doi.org/10.1016/j.ocemod.2012.11.002, 2013.

Ivanovic, R. F., Valdes, P. J., Gregoire, L., Flecker, R., and Gutjahr, M.: Sensitivity of modern climate to the presence, strength and salinity of Mediterranean-Atlantic exchange in a global general circulation model, Climate Dynamics, 42, 859–877, https://doi.org/10.1007/s00382-013-1680-5, 2014.

Jeandel, C.: Concentration and isotopic composition of Nd in the South Atlantic Ocean, Earth and Planetary Science Letters, 117, 581–591, https://doi.org/10.1016/0012-821X(93)90104-H, 1993.

Jeandel, C. and Oelkers, E. H.: The influence of terrigenous particulate material dissolution on ocean chemistry and global element cycles, Chemical Geology, 395, 50–66, https://doi.org/10.1016/j.chemgeo.2014.12.001, 2015.

Jeandel, C., Bishop, J. K., and Zindler, A.: Exchange of neodymium and its isotopes between seawater and small and large particles in the Sargasso Sea, Geochimica et Cosmochimica Acta, 59, 535–547, https://doi.org/10.1016/0016-7037(94)00367-U, 1995.

Jeandel, C., Arsouze, T., Lacan, F., Téchiné, P., and Dutay, J. C.: Isotopic Nd compositions and concentrations of the lithogenic inputs into the ocean: A compilation, with an emphasis on the margins, Chemical Geology, 239, 156–164, https://doi.org/10.1016/j.chemgeo.2006.11.013, 2007.

Jia, Y.: Formation of an Azores Current Due to Mediterranean Overflow in a Modeling Study of the North Atlantic, Journal of Physical Oceanography, 30, 2342–2358, 2000.

Jiménez-Espejo, F., Pardos-Gené, M., Martínez-Ruiz, F., García-Alix, A., van de Flierdt, T., Toyofuku, T., Bahr, A., and Kreissig, K.: Geochemical evidence for intermediate water circulation in the westernmost Mediterranean over the last 20kyrBP and its impact on the Mediterranean Outflow, Global and Planetary Change, 135, 38–46, https://doi.org/10.1016/j.gloplacha.2015.10.001, 2015.

Kallel, N. and Labeyrie, L.: Enhanced rainfall in the Mediterranean region during the last Sapropel Event, Oceanologica Acta, 20, 697–7712, https://www.researchgate.net/publication/277157107, 1997.

Khélifi, N., Samthein, M., Andersen, N., Blanz, T., Frank, M., Garbe-Schönberg, D., Haley, B. A., Stumpf, R., and Weinelt, M.: A major and long-term Pliocene intensification of the Mediterranean outflow, 3.5-3.3 Ma ago, Geology, 37, 811–814, https://doi.org/10.1130/G30058A.1, 2009.

Kurzweil, F., Gutjahr, M., Vance, D., and Keigwin, L.: Authigenic Pb isotopes from the Laurentian Fan: Changes in chemical weathering and patterns of North American freshwater runoff during the last deglaciation, Earth and Planetary Science Letters, 299, 458–465, https://doi.org/10.1016/j.epsl.2010.09.031, 2010.

Lacan, F. and Jeandel, C.: Tracing Papua New Guinea imprint on the central Equatorial Pacific Ocean using neodymium isotopic compositions and Rare Earth Element patterns, Earth and Planetary Science Letters, 186, 497–512, https://doi.org/10.1016/S0012-821X(01)00263-1, 2001.

Lacan, F. and Jeandel, C.: Neodymium isotopic composition and rare earth element concentrations in the deep and intermediate Nordic Seas: Constraints on the Iceland Scotland Overflow Water signature, Geochemistry, Geophysics, Geosystems, 5, https://doi.org/10.1029/2004GC000742, 2004a.

Lacan, F. and Jeandel, C.: Denmark Strait water circulation traced by heterogeneity in neodymium isotopic compositions, Deep-Sea Research Part I: Oceanographic Research Papers, 51, 71–82, https://doi.org/10.1016/j.dsr.2003.09.006, 2004b.

Lacan, F. and Jeandel, C.: Subpolar mode water formation traced by neodymium isotopic composition, Geophysical Research Letters, 31, https://doi.org/10.1029/2004GL019747, 2004c.

Lacan, F. and Jeandel, C.: Acquisition of the neodymium isotopic composition of the North Atlantic Deep Water, Geochemistry, Geophysics, Geosystems, 6, https://doi.org/10.1029/2005GC000956, 2005a.

Lacan, F. and Jeandel, C.: Acquisition of the neodymium isotopic composition of the North Atlantic Deep Water, Geochemistry, Geophysics, Geosystems, 6, n/a–n/a, https://doi.org/10.1029/2005GC000956, 2005b.

Lacan, F. and Jeandel, C.: Neodymium isotopes as a new tool for quantifying exchange fluxes at the continent-ocean interface, Earth and Planetary Science Letters, 232, 245–257, https://doi.org/10.1016/j.epsl.2005.01.004, 2005c.

Lambelet, M., van de Flierdt, T., Crocket, K., Rehkämper, M., Kreissig, K., Coles, B., Rijkenberg, M. J., Gerringa, L. J., de Baar, H. J., and Steinfeldt, R.: Neodymium isotopic composition and concentration in the western North Atlantic Ocean: Results from the GEOTRACES GA02 section, Geochimica et Cosmochimica Acta, 177, 1–29, https://doi.org/10.1016/j.gca.2015.12.019, 2016.

Lavender, K. L., Brechner Owens, W., and Davis, R. E.: The mid-depth circulation of the subpolar North Atlantic Ocean as measured by subsurface floats, Deep-Sea Research Part I: Oceanographic Research Papers, 52, 767–785, https://doi.org/10.1016/j.dsr.2004.12.007, 2005.

Lippold, J., Gutjahr, M., Blaser, P., Christner, E., de Carvalho Ferreira, M. L., Mulitza, S., Christl, M., Wombacher, F., Böhm, E., Antz, B., Cartapanis, O., Vogel, H., and Jaccard, S. L.: Deep water provenance and dynamics of the (de)glacial Atlantic meridional overturning circulation, Earth and Planetary Science Letters, 445, 68–78, https://doi.org/10.1016/J.EPSL.2016.04.013, https://www.sciencedirect.com/science/article/pii/S0012821X16301698, 2016.

Lozier, M. S. and Stewart, N. M.: On the temporally varying northward penetration of mediterranean overflow water and eastward penetration of Labrador sea water, Journal of Physical Oceanography, 38, 2097–2103, https://doi.org/10.1175/2008JPO3908.1, https://journals.ametsoc.org/view/journals/phoc/38/9/2008jpo3908.1.xml, 2008.

Madec, G. and Crepon, M.: Thermohaline-driven deep water formation in the northwestern mediterranean sea, Elsevier Oceanography Series, 57, 241–265, https://doi.org/10.1016/S0422-9894(08)70071-0, 1991.

Madec, G. and NEMO-Team.: Note du Pole de modélisation, Institut Pierre-Simon Laplace (IPSL), France, NEMO ocean engine, 27, https://doi.org/ISSN N1288-1619, 2008.

McManus, J. F., Francois, R., Gherardi, J.-M., Keigwin, L. D., and Brown-Leger, S.: Collapse and rapid resumption of Atlantic meridional circulation linked to deglacial climate changes, Nature, 428, 834–837, https://doi.org/10.1038/nature02494, http://www.nature.com/doifinder/10.1038/nature02494, 2004.

Mercone, D., Thomson, J., Croudace, I. W., Siani, G., Paterne, M., and Troelstra, S.: Duration of S1, the most recent sapropel in the eastern Mediterranean Sea, as indicated by accelerator mass spectrometry radiocarbon and geochemical evidence, Paleoceanography, 15, 336–347, https://doi.org/10.1029/1999PA000397, 2000.

Montero-Serrano, J. C., Frank, N., Colin, C., Wienberg, C., and Eisele, M.: The climate influence on the mid-depth Northeast Atlantic gyres viewed by cold-water corals, Geophysical Research Letters, 38, https://doi.org/10.1029/2011GL048733, 2011.

Montero-Serrano, J. C., Frank, N., Tisnérat-Laborde, N., Colin, C., Wu, C. C., Lin, K., Shen, C. C., Copard, K., Orejas, C., Gori, A., De Mol, L., Van Rooij, D., Reverdin, G., and Douville, E.: Decadal changes in the mid-depth water mass dynamic of the Northeastern Atlantic margin (Bay of Biscay), Earth and Planetary Science Letters, 364, 134–144, https://doi.org/10.1016/j.epsl.2013.01.012, 2013.

Moreno, A., Cacho, I., Canals, M., Grimalt, J. O., Sánchez-Goñi, M. F., Shackleton, N., and Sierro, F. J.: Links between marine and atmospheric processes oscillating on a millennial time-scale. A multi-proxy study of the last 50,000 yr from the Alboran Sea (Western Mediterranean Sea), Quaternary Science Reviews, 24, 1623–1636, https://doi.org/10.1016/j.quascirev.2004.06.018, 2005.

Myers, P. G., Haines, K., and Rohling, E. J.: Modeling the paleocirculation of the Mediterranean: The last glacial maximum and the Holocene with emphasis on the formation of sapropel S1, Paleoceanography, 13, 586–606, https://doi.org/10.1029/98PA02736, 1998.

New, A. L. and Smythe-Wright, D.: Aspects of the circulation in the rockall trough, Continental Shelf Research, 21, 777–810, https://doi.org/10.1016/S0278-4343(00)00113-8, 2001.

New, A. L., Jia, Y., Coulibaly, M., and Dengg, J.: On the role of the Azores Current in the ventilation of the North Atlantic Ocean, Progress in Oceanography, 48, 163–194, https://doi.org/10.1016/S0079-6611(01)00004-0, 2001.

O'Brien, S. R., Mayewski, P. A., Meeker, L. D., Meese, D. A., Twickler, M. S., and Whitlow, S. I.: Complexity of Holocene Climate as Reconstructed from a Greenland Ice Core, https://doi.org/10.2307/2888820, https://www.jstor.org/stable/2888820, 1995.

Penaud, A., Eynaud, F., Sánchez-Goñi, M., Malaizé, B., Turon, J. L., and Rossignol, L.: Contrasting sea-surface responses between the western Mediterranean Sea and eastern subtropical latitudes of the North Atlantic during abrupt climatic events of MIS 3, Marine Micropaleontology, 80, 1–17, https://doi.org/10.1016/j.marmicro.2011.03.002, 2011.

Penny Holliday, N., Pollard, R. T., Read, J. F., and Leach, H.: Water mass properties and fluxes in the Rockall Trough, 1975-1998, Deep-Sea Research Part I: Oceanographic Research Papers, 47, 1303–1332, https://doi.org/10.1016/S0967-0637(99)00109-0, 2000.

Piepgras, D. J. and Wasserburg, G. J.: Influence of the Mediterranean Outflow on the isotopic composition of neodymium in waters of the North Atlantic, Journal of Geophysical Research, 88, 5997–6006, https://doi.org/10.1029/JC088iC10p05997, 1983.

Piepgras, D. J. and Wasserburg, G. J.: Rare earth element transport in the western North Atlantic inferred from Nd isotopic observations, Geochimica et Cosmochimica Acta, 51, 1257–1271, https://doi.org/10.1016/0016-7037(87)90217-1, 1987.

Rahmstorf, S.: Influence of mediterranean outflow on climate, Eos, Transactions American Geophysical Union, 79, 281–281, https://doi.org/10.1029/98EO00208, http://doi.wiley.com/10.1029/98EO00208, 1998.

Rempfer, J., Stocker, T. F., Joos, F., Dutay, J. C., and Siddall, M.: Modelling Nd-isotopes with a coarse resolution ocean circulation model: Sensitivities to model parameters and source/sink distributions, Geochimica et Cosmochimica Acta, 75, 5927–5950, https://doi.org/10.1016/j.gca.2011.07.044, 2011.

Renssen, H., Goosse, H., Crosta, X., and Roche, D. M.: Early holocene laurentide ice sheet deglaciation causes cooling in the high-latitude southern hemisphere through oceanic teleconnection, Paleoceanography, 25, https://doi.org/10.1029/2009PA001854, 2010.

Repschläger, J., Garbe-Schönberg, D., Weinelt, M., and Schneider, R.: Holocene evolution of the North Atlantic subsurface transport, Climate of the Past, 13, 333–344, https://doi.org/10.5194/cp-13-333-2017, 2017.

Revel, M., Ducassou, E., Grousset, F. E., Bernasconi, S. M., Migeon, S., Revillon, S., Mascle, J., Murat, A., Zaragosi, S., and Bosch, D.: 100,000 Years of African monsoon variability recorded in sediments of the Nile margin, Quaternary Science Reviews, 29, 1342–1362, https://doi.org/10.1016/j.quascirev.2010.02.006, 2010.

Revel, M., Colin, C., Bernasconi, S., Combourieu-Nebout, N., Ducassou, E., Grousset, F. E., Rolland, Y., Migeon, S., Bosch, D., Brunet, P., Zhao, Y., and Mascle, J.: 21,000 Years of Ethiopian African monsoon variability recorded in sediments of the western Nile deep-sea fan, Regional Environmental Change, 14, 1685–1696, https://doi.org/10.1007/s10113-014-0588-x, 2014.

Roberts, N. L. and Piotrowski, A. M.: Radiogenic Nd isotope labeling of the northern NE Atlantic during MIS 2, Earth and Planetary Science Letters, 423, 125–133, https://doi.org/10.1016/j.epsl.2015.05.011, 2015.

Roberts, N. L., Piotrowski, A. M., McManus, J. F., and Keigwin, L. D.: Synchronous deglacial overturning and water mass source changes, Science, 327, 75–78, https://doi.org/10.1126/science.1178068, 2010.

Roche, D. M., Wiersma, A. P., and Renssen, H.: A systematic study of the impact of freshwater pulses with respect to different geographical locations, Climate Dynamics, 34, 997–1013, https://doi.org/10.1007/s00382-009-0578-8, 2010.

Rogerson, M., Rohlin, E. J., and Weaver, P. P.: Promotion of meridional overturning by Mediterranean-derived salt during the last deglaciation, Paleoceanography, 21, https://doi.org/10.1029/2006PA001306, 2006.

Rogerson, M., Colmenero-Hidalgo, E., Levine, R. C., Rohling, E. J., Voelker, A. H., Bigg, G. R., Schönfeld, J., Cacho, I., Sierro, F. J., Löwemark, L., Reguera, M. I., De Abreu, L., and Garrick, K.: Enhanced Mediterranean-Atlantic exchange during Atlantic freshening phases, Geochemistry, Geophysics, Geosystems, 11, https://doi.org/10.1029/2009GC002931, 2010.

Rohling, E., Mayewski, P., Abu-Zied, R., Casford, J., and Hayes, A.: Holocene atmosphere-ocean interactions: Records from Greenland and the Aegean sea, Climate Dynamics, 18, 587–594, https://doi.org/10.1007/s00382-001-0194-8, 2002.

Rohling, E. J.: Review and new aspects concerning the formation of eastern Mediterranean sapropels, Marine Geology, 122, 1–28, https://doi.org/10.1016/0025-3227(94)90202-X, 1994.

Rohling, E. J., Grant, K., Bolshaw, M., Roberts, A. P., Siddall, M., Hemleben, C., and Kucera, M.: Antarctic temperature and global sea level closely coupled over the past five glacial cycles, Nature Geoscience, 2, 500–504, https://doi.org/10.1038/ngeo557, 2009.

Rohling, E. J., Marino, G., and Grant, K. M.: Mediterranean climate and oceanography, and the periodic development of anoxic events (sapropels), https://doi.org/10.1016/j.earscirev.2015.01.008, 2015.

Rossignol-Strick, M., Nesteroff, W., Olive, P., and Vergnaud Grazzini, C.: After the deluge: Mediterranean stagnation and sapropel formation, Nature, 295, 105–110, https://doi.org/10.1038/295105a0, 1982.

Rossignol-Strick, M., Planchais, N., Paterne, M., and Duzer, D.: Vegetation dynamics and climate during the deglaciation in the south Adriatic basin from a marine record, Quaternary Science Reviews, 11, 415–423, https://doi.org/10.1016/0277-3791(92)90023-2, 1992.

Roullet, G. and Madec, G.: Salt conservation, free surface, and varying levels: A new formulation for ocean general circulation models, Journal of Geophysical Research: Oceans, 105, 23 927–23 942, https://doi.org/10.1029/2000jc900089, 2000.

Scrivner, A. E., Vance, D., and Rohling, E. J.: New neodymium isotope data quantify Nile involvement in Mediterranean anoxic episodes, Geology, 32, 565–568, https://doi.org/10.1130/G20419.1, 2004.

Sepulchre, P., Arsouze, T., Donnadieu, Y., Dutay, J. C., Jaramillo, C., Le Bras, J., Martin, E., Montes, C., and Waite, a. J.: Consequences of shoaling of the Central American Seaway determined from modeling Nd isotopes, Paleoceanography, 29, 176–189, https://doi.org/10.1002/2013PA002501, 2014.

Siddall, M., Khatiwala, S., van de Flierdt, T., Jones, K., Goldstein, S. L., Hemming, S., and Anderson, R. F.: Towards explaining the Nd paradox using reversible scavenging in an ocean general circulation model, Earth and Planetary Science Letters, 274, 448–461, https://doi.org/10.1016/j.epsl.2008.07.044, 2008.

Sierro, F. J., Hodell, D. A., Curtis, J. H., Flores, J. A., Reguera, I., Colmenero-Hidalgo, E., Bárcena, M. A., Grimalt, J. O., Cacho, I., Frigola, J., and Canals, M.: Impact of iceberg melting on Mediterranean thermohaline circulation during Heinrich events, Paleoceanography, 20, 1–13, https://doi.org/10.1029/2004PA001051, 2005.

Spivack, A. J. and Wasserburg, G. J.: Neodymium isotopic composition of the Mediterranean outflow and the eastern North Atlantic, Geochimica et Cosmochimica Acta, 52, 2767–2773, https://doi.org/10.1016/0016-7037(88)90144-5, 1988.

Staines-Urías, F., Kuijpers, A., and Korte, C.: Evolution of subpolar North Atlantic surface circulation since the early Holocene inferred from planktic foraminifera faunal and stable isotope records, Quaternary Science Reviews, 76, 66–81, https://doi.org/10.1016/j.quascirev.2013.06.016, 2013.

Stichel, T., Frank, M., Rickli, J. D., Hathorne, E., Haley, B. A., Jeandel, C., and Pradoux, C.: Hafnium and neodymium in surface waters of the Atlantic sector of the Southern Ocean, https://doi.org/10.1594/PANGAEA.786906, 2012.

Stratford, K., Williams, R. G., and Myers, P. G.: Impact of the circulation on sapropel formation in the eastern Mediterranean, Global Biogeochemical Cycles, 14, 683–695, https://doi.org/10.1029/1999GB001157, 2000.

Struglia, M. V., Mariotti, A., and Filograsso, A.: River discharge into the Mediterranean sea: Climatology and aspects of the observed variability, Journal of Climate, 17, 4740–4751, https://doi.org/10.1175/JCLI-3225.1, 2004.

Swingedouw, D., Colin, C., Eynaud, F., Ayache, M., and Zaragosi, S.: Impact of freshwater release in the Mediterranean Sea on the North Atlantic climate, Climate Dynamics, https://doi.org/10.1007/s00382-019-04758-5, 2019.

Tachikawa, K., Jeandel, C., and Roy-Barman, M.: A new approach to the Nd residence time in the ocean: the role of atmospheric inputs, Earth and Planetary Science Letters, 170, 433–446, https://doi.org/10.1016/S0012-821X(99)00127-2, 1999.

Tachikawa, K., Athias, V., and Jeandel, C.: Neodymium budget in the modern ocean and paleo-oceanographic implications, Journal of Geophysical Research, 108, 3254, https://doi.org/10.1029/1999JC000285, http://doi.wiley.com/10.1029/1999JC000285, 2003.

Tachikawa, K., Roy-Barman, M., Michard, A., Thouron, D., Yeghicheyan, D., and Jeandel, C.: Neodymium isotopes in the Mediterranean Sea: comparison between seawater and sediment signals, Geochimica et Cosmochimica Acta, 68, 3095–3106, https://doi.org/10.1016/j.gca.2004.01.024, http://linkinghub.elsevier.com/retrieve/pii/S0016703704001231, 2004.

Tachikawa, K., Arsouze, T., Bayon, G., Bory, A., Colin, C., Dutay, J. C., Frank, N., Giraud, X., Gourlan, A. T., Jeandel, C., Lacan, F., Meynadier, L., Montagna, P., Piotrowski, A. M., Plancherel, Y., Pucéat, E., Roy-Barman, M., and Waelbroeck, C.: The large-scale evolution of neodymium isotopic composition in the global modern and Holocene ocean revealed from seawater and archive data, Chemical Geology, 457, 131–148, https://doi.org/10.1016/j.chemgeo.2017.03.018, 2017.

Thornalley, D. J., Elderfield, H., and McCave, I. N.: Holocene oscillations in temperature and salinity of the surface subpolar North Atlantic, Nature, 457, 711–714, https://doi.org/10.1038/nature07717, 2009.

Thornalley, D. J. R., Barker, S., Broecker, W. S., Elderfield, H., and McCave, I. N.: The deglacial evolution of North Atlantic deep convection., Science (New York, N.Y.), 331, 202–5, https://doi.org/10.1126/science.1196812, http://www.ncbi.nlm.nih.gov/pubmed/21233385, 2011.

Thornalley, D. J. R., Blaschek, M., Davies, F. J., Praetorius, S., Oppo, D. W., Mcmanus, J. F., Hall, I. R., Kleiven, H., Renssen, H., and Mccave, I. N.: Long-term variations in Iceland–Scotland overflow strength during the Holocene Geoscientific Instrumentation Methods and Data Systems Long-term variations in Iceland–Scotland overflow strength during the Holocene, Clim.

Past, 95194, 2073–2084, https://doi.org/10.5194/cp-9-2073-2013, http://hdl.handle.net/1957/46955http://cdss.library.oregonstate.edu/sa-termsofusewww.clim-past.net/9/2073/2013/, 2013.

Tierney, J. E., Pausata, F. S. R., and DeMenocal, P. B.: Rainfall regimes of the Green Sahara, Science Advances, 3, e1601 503, https://doi.org/10.1126/sciadv.1601503, 2017.

Toucanne, S., Soulet, G., Freslon, N., Silva Jacinto, R., Dennielou, B., Zaragosi, S., Eynaud, F., Bourillet, J. F., and Bayon, G.: Millennial-scale fluctuations of the European Ice Sheet at the end of the last glacial, and their potential impact on global climate, Quaternary Science Reviews, 123, 113–133, https://doi.org/10.1016/j.quascirev.2015.06.010, 2015.

Tsimplis, M. N. and Bryden, H. L.: Estimation of the transports through the Strait of Gibraltar, Deep-Sea Research Part I: Oceanographic Research Papers, 47, 2219–2242, https://doi.org/10.1016/S0967-0637(00)00024-8, 2000.

Vadsaria, T., Ramstein, G., Dutay, J. C., Li, L., Ayache, M., and Richon, C.: Simulating the Occurrence of the Last Sapropel Event (S1): Mediterranean Basin Ocean Dynamics Simulations Using Nd Isotopic Composition Modeling, Paleoceanography and Paleoclimatology, 34, 237–251, https://doi.org/10.1029/2019PA003566, 2019.

Van Aken, H. M. and de Jong, M. F.: Hydrographic variability of Denmark Strait Overflow Water near Cape Farewell with multi-decadal to weekly time scales, Deep-Sea Research Part I: Oceanographic Research Papers, 66, 41–50, https://doi.org/10.1016/j.dsr.2012.04.004, 2012.

Vance, D., Scrivner, A. E., Beney, P., Staubwasser, M., Henderson, G. M., and Slowey, N. C.: The use of foraminifera as a record of the past neodymium isotope composition of seawater, Paleoceanography, 19, n/a—-n/a, https://doi.org/10.1029/2003PA000957, 2004.

Voelker, A. H., Lebreiro, S. M., Schönfeld, J., Cacho, I., Erlenkeuser, H., and Abrantes, F.: Mediterranean outflow strengthening during northern hemisphere coolings: A salt source for the glacial Atlantic?, Earth and Planetary Science Letters, 245, 39–55, https://doi.org/10.1016/j.epsl.2006.03.014, 2006.

Wu, J., Pahnke, K., Böning, P., Wu, L., Michard, A., and de Lange, G. J.: Divergent Mediterranean seawater circulation during Holocene sapropel formation – Reconstructed using Nd isotopes in fish debris and foraminifera, Earth and Planetary Science Letters, 511, 141–153, https://doi.org/10.1016/j.epsl.2019.01.036, 2019.

Xie, R. C., Marcantonio, F., and Schmidt, M. W.: Deglacial variability of Antarctic Intermediate Water penetration into the North Atlantic from authigenic neodymium isotope ratios, Paleoceanography, 27, https://doi.org/10.1029/2012PA002337, 2012.

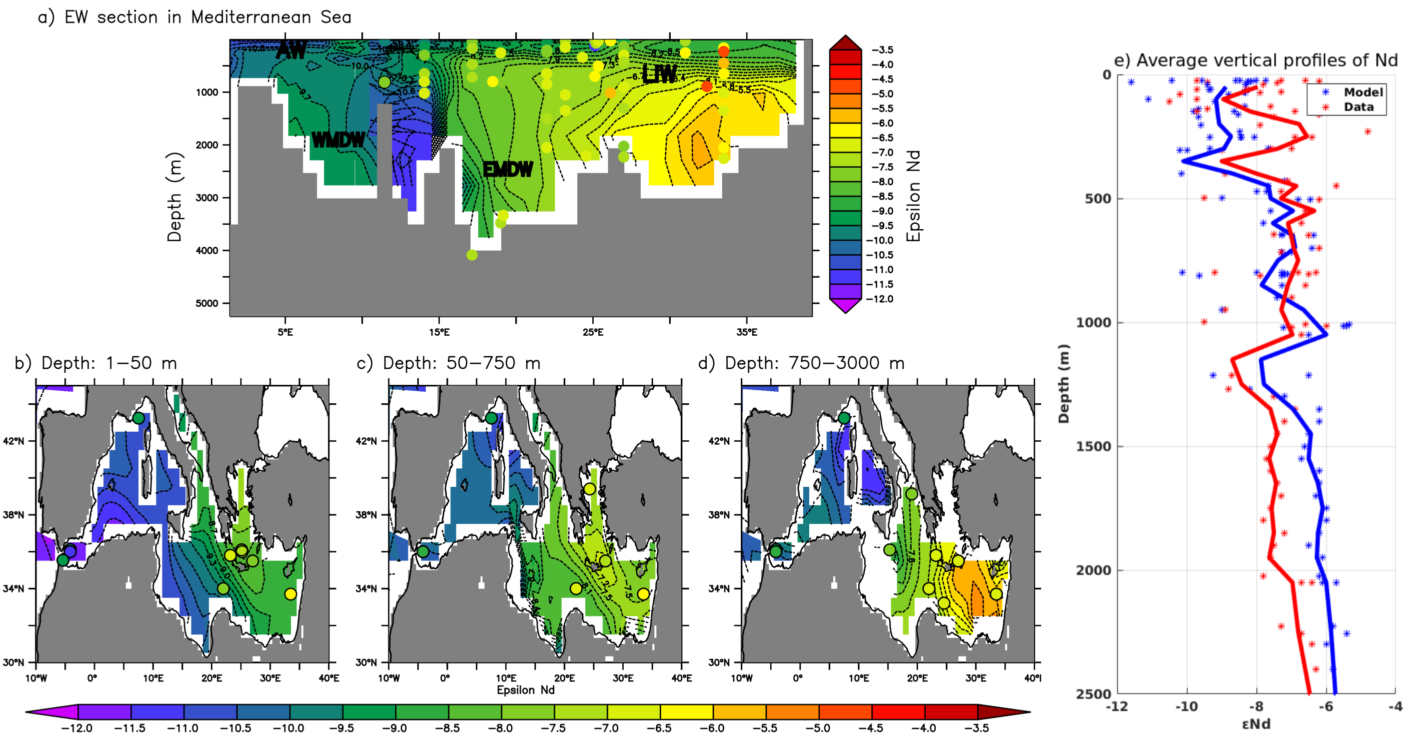

Figure 1. Model-data comparison of $\varepsilon_{\mathrm{Nd}}$ for the Mediterranean Sea from control simulation (averaged over last 100 years). Upper line East-West section **(a)**. Lower panel: horizontal maps for surface waters **(b)**, intermediate waters **(c)**, and deep waters **(d)**. Color-filled dots represent *in situ* observations from Tachikawa et al. (2004), Vance et al. (2004) and Henry et al. (1994). Both use the same colour scale. LIW (Levantine intermediate water), AW (Atlantic Waters), WMDW (Western Mediterranean Deep Water) EMDW (Eastern Mediterranean Deep Water) appears in panel a). **e)** Comparison of average vertical profiles of Nd isotopic signature ($\varepsilon_{\mathrm{Nd}}$) from control run in the whole Mediterranean Sea. Model results are in blue, while red indicates the in situ data from Tachikawa et al. (2004), Vance et al. (2004) and Henry et al. (1994).

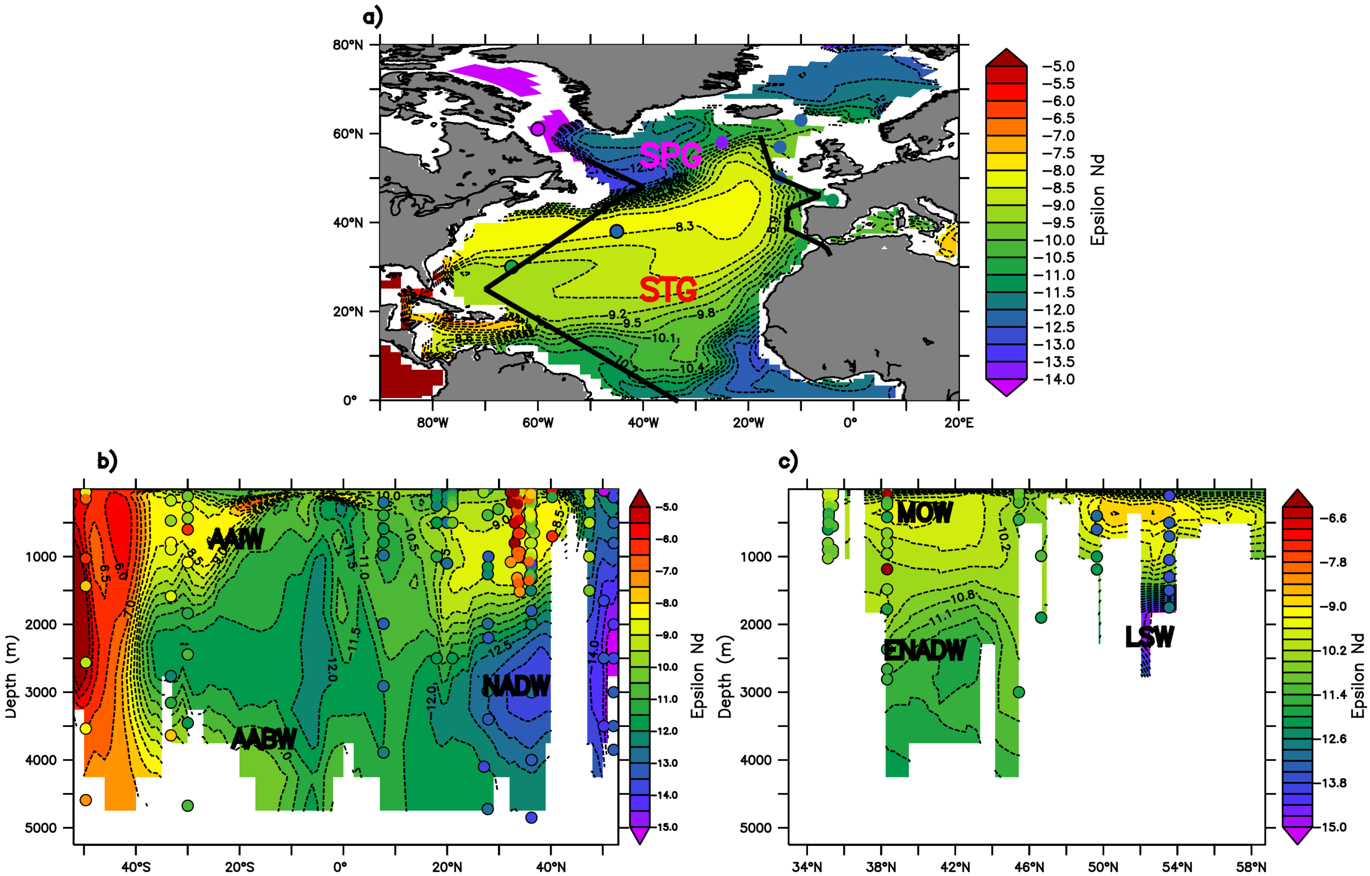

Figure 2. Model-data comparison of ε_{Nd} for the North Atlantic basin from control simulation (averaged over last 100 years), **a)** horizontal distribution of ε_{Nd} in the mid-depth waters (750 m), **b)** section along the north to equatorial western Atlantic basin, **c)** section along a latitudinal transect in the western European margin. colour-filled dots represent *in situ* observations from Dubois-Dauphin et al. (2017) and Lambelet et al. (2016). Both use the same colour scale. AAIW (Antarctic Intermediate Water), AABW (Antarctic Bottom Water), NADW (North Atlantic Deep-Water), MOW (Mediterranean overflow water), LSW (Labrador Sea Water), ENADW (North East Atlantic Deep-Water), SPG (Subpolar Gyre), STG (subtropical gyre) .

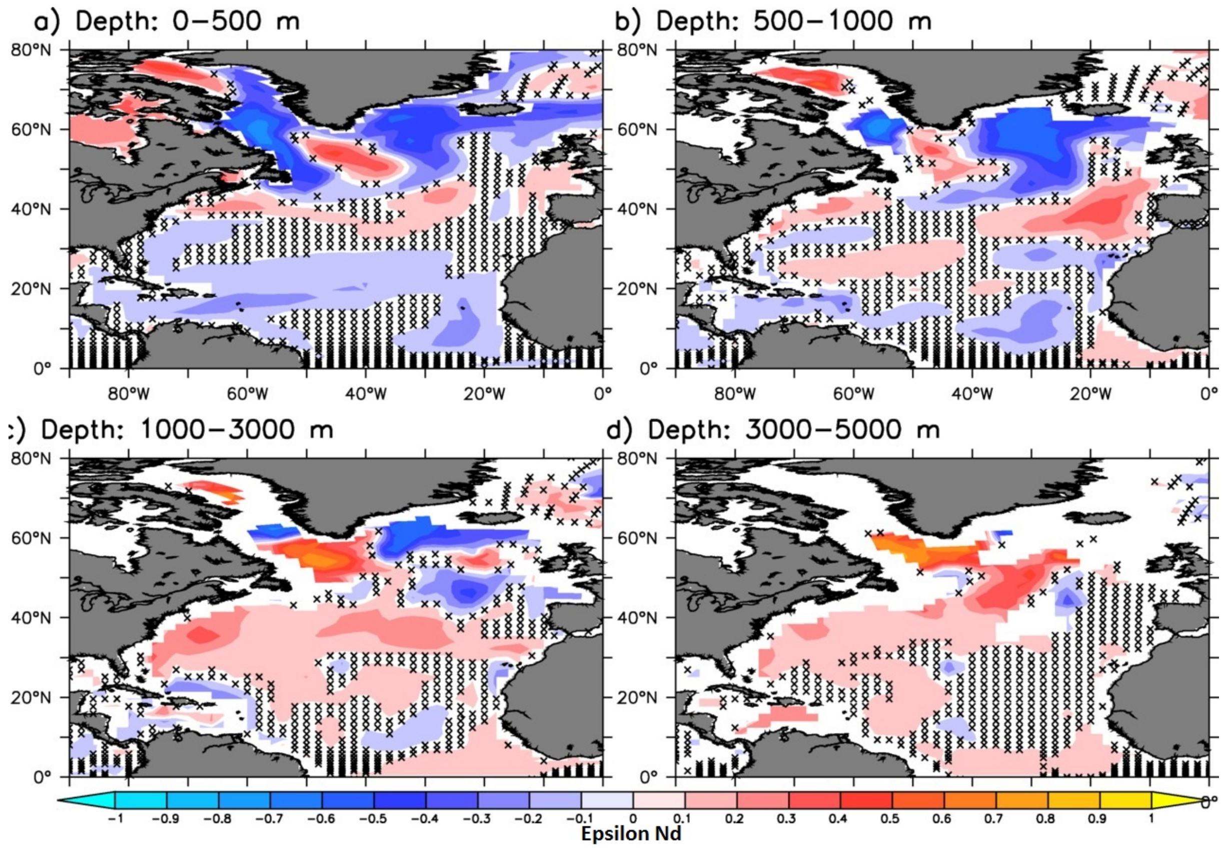

Figure 3. Map of time correlation between the $\varepsilon_{\mathrm{Nd}}$ and subpolar gyre index (defined as the maximum of the barotropic stream function) from the control simulation averaged over different depth ranges: 0-500m in **a)**, 500-1000m in **b)**, 1000-3000m in **c)** and 3000-5000m in **d)**. The non-significant zones for the regression at 95% level are marked with a black cross.

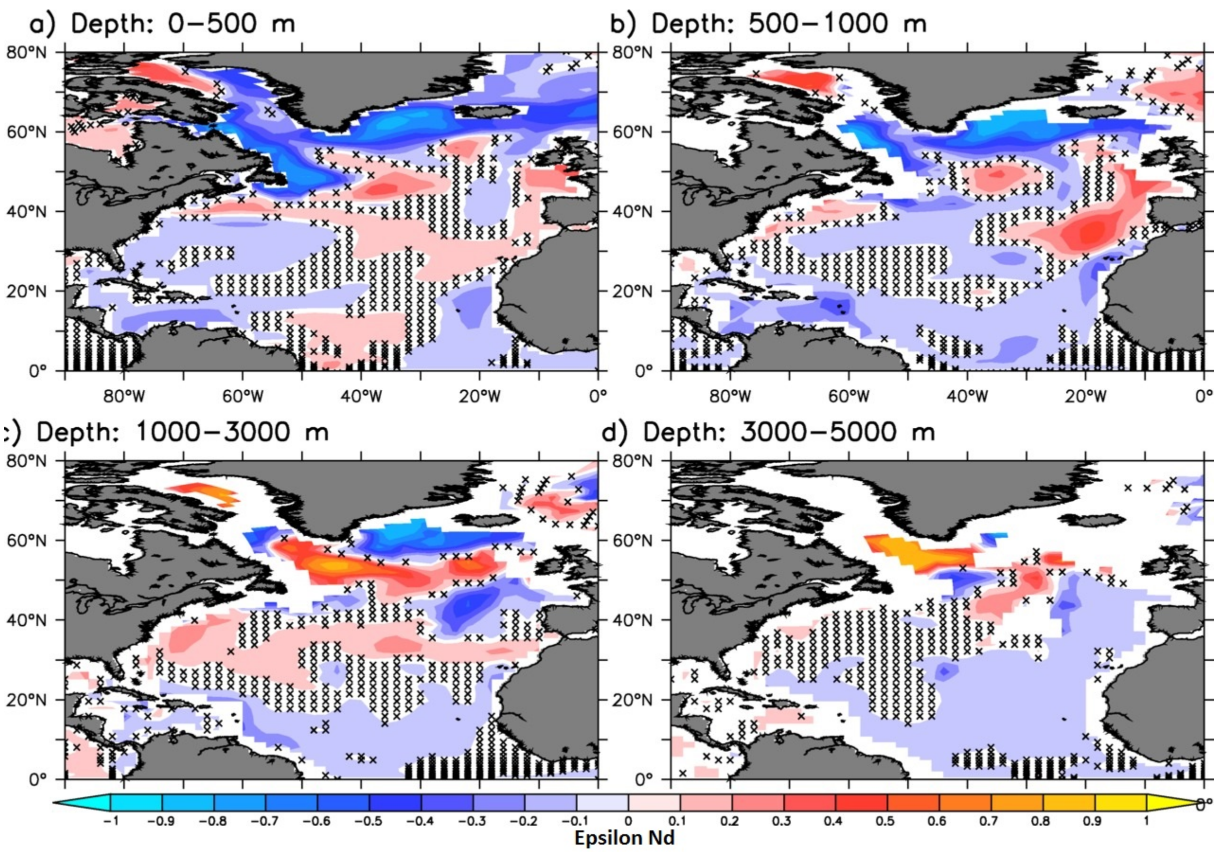

Figure 4. Same as Figure 3 but with AMOC index.

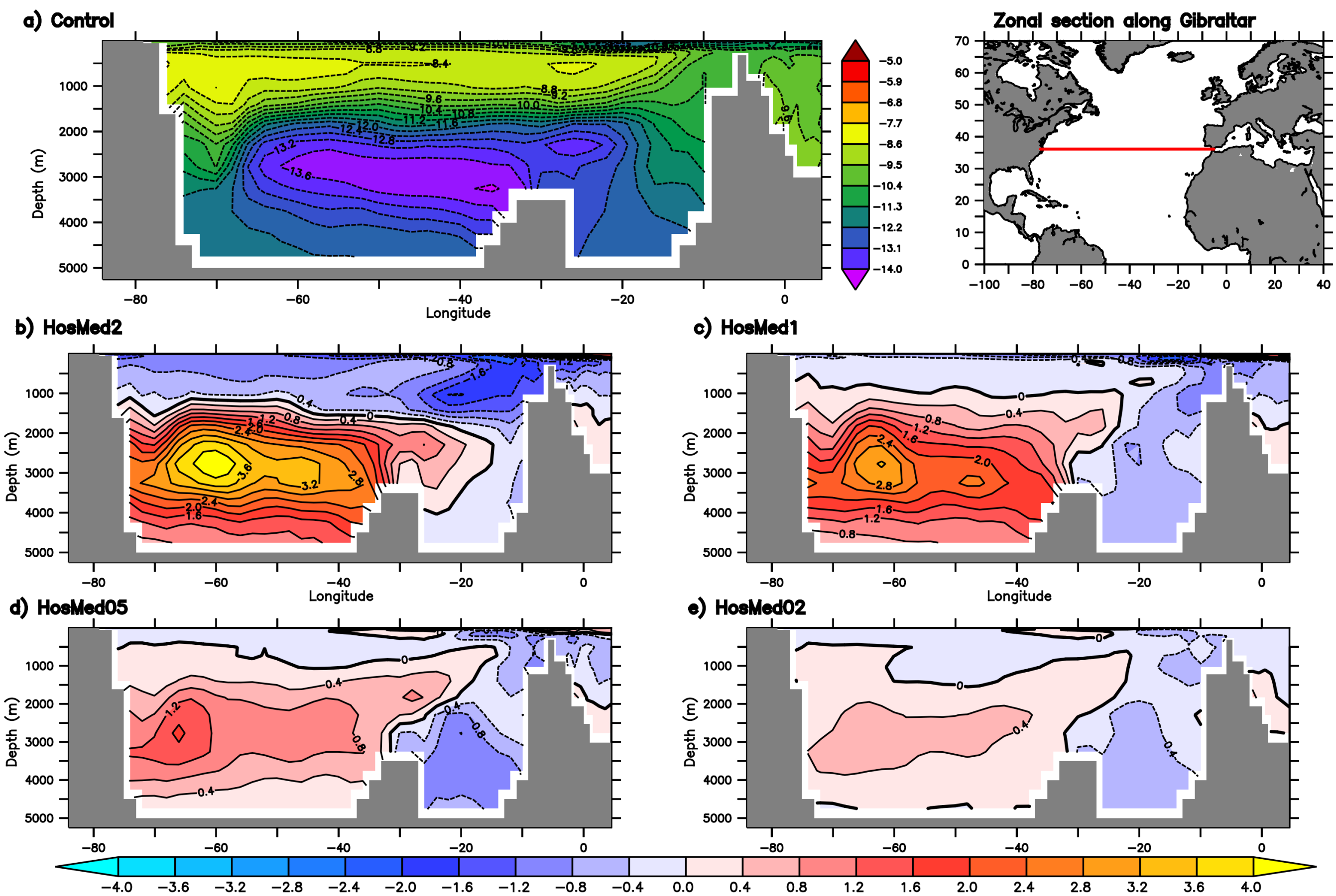

Figure 5. a) $\varepsilon_{\mathrm{Nd}}$ in the control simulation (averaged over 1000 years) along a longitude-depth section at around 36°N (*cf.* zonal section plot), latitude of the Gibraltar Strait. **b)**, **c)**, **d)** and **e)** $\varepsilon_{\mathrm{Nd}}$ anomalies between control simulation and HosMed2, HosMed1, HosMed05 and HosMed02 respectively.

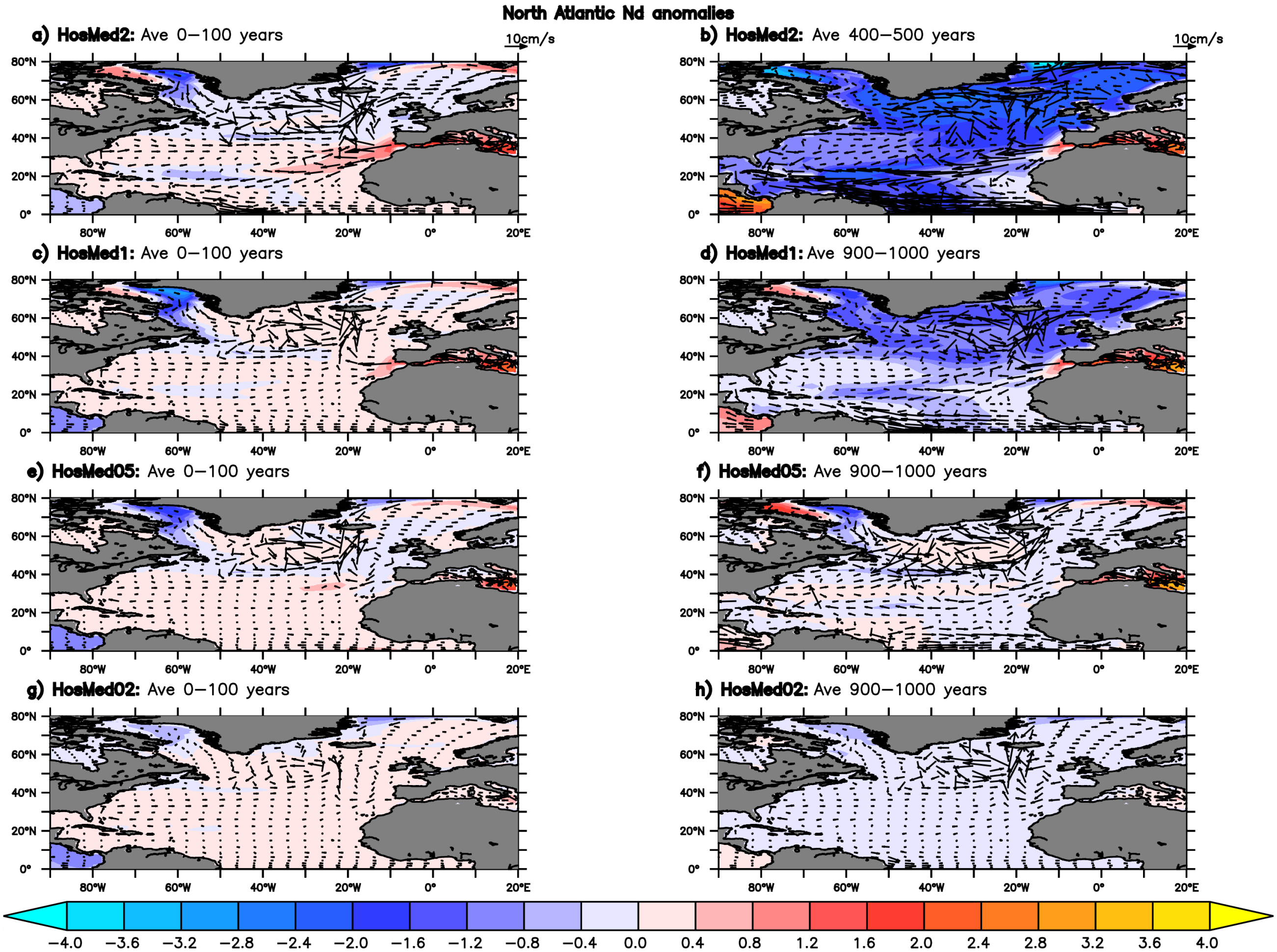

Figure 6. $\varepsilon_{\mathrm{Nd}}$ anomaly from control simulation computed over the first 100 years of simulation on the left and last 100 years on the right. First line is for HosMed2, second for HosMed1, third for HosMed05 and fourth for HosMed02. Superimposed are the velocity anomalies from control simulation averaged over the first 100 meters of the ocean (in cm/s).

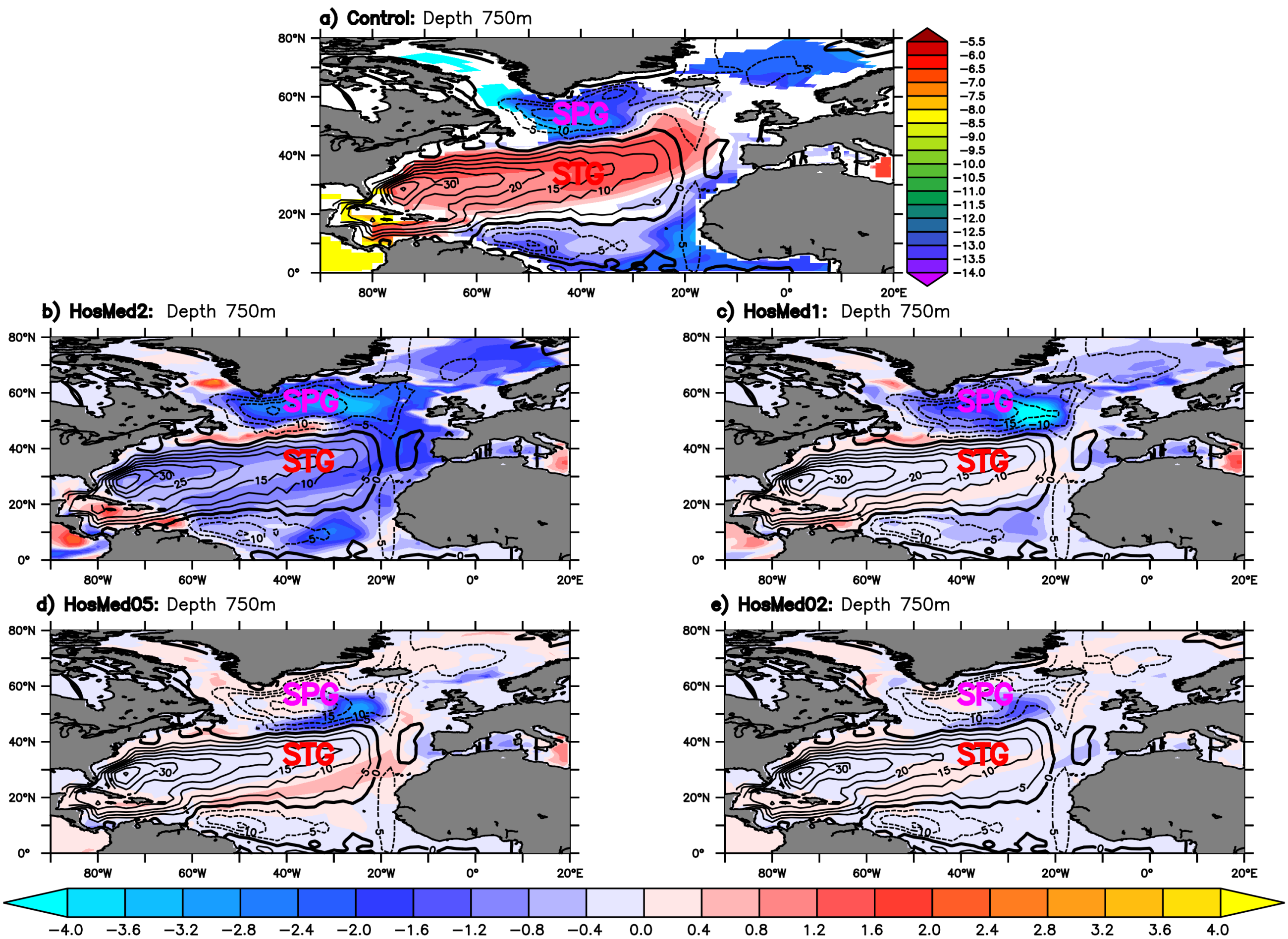

Figure 7. a) Horizontal maps of $\varepsilon_{\mathrm{Nd}}$ distribution at 750 m depth in the North Atlantic basin. **b)**, **c)**, **d)** and **e)** $\varepsilon_{\mathrm{Nd}}$ anomalies between control simulation and HosMed2, HosMed1, HosMed05 and HosMed02, respectively. Shown in contour the mean of the barotropic stream function in the control simulation averaged over 1000 years SPG (Subpolar Gyre), STG (subtropical gyre). We only show the differences significant at the 95% level following a student t-test.

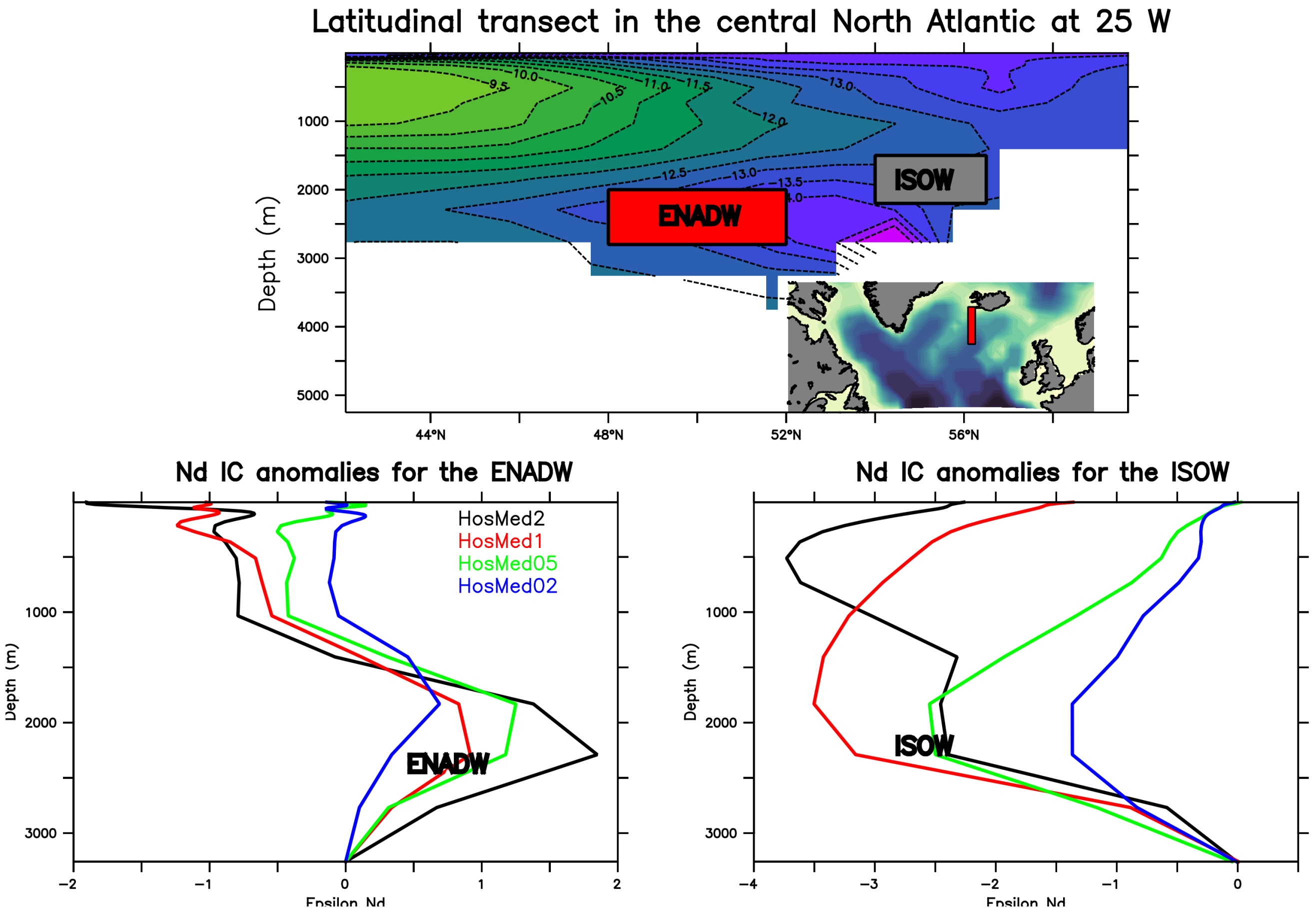

Figure 8. Comparison of Nd isotopic signature anomalies associated with the Iceland-Scotland Overflow Water (ISOW, at 56 °N 25 °W) identified between 2000 and 2600 m depth south of Iceland (Harvey and Theodorou, 1986) and the North Eastern Atlantic Deep Water (NEADW, at 50 °N 25 °W) between 2000 and 3000 m (Van Aken and de Jong, 2012), in HosMed2 (in black), HosMed1 (in red), HosMed05 (in green), and HosMed02 (in blue).

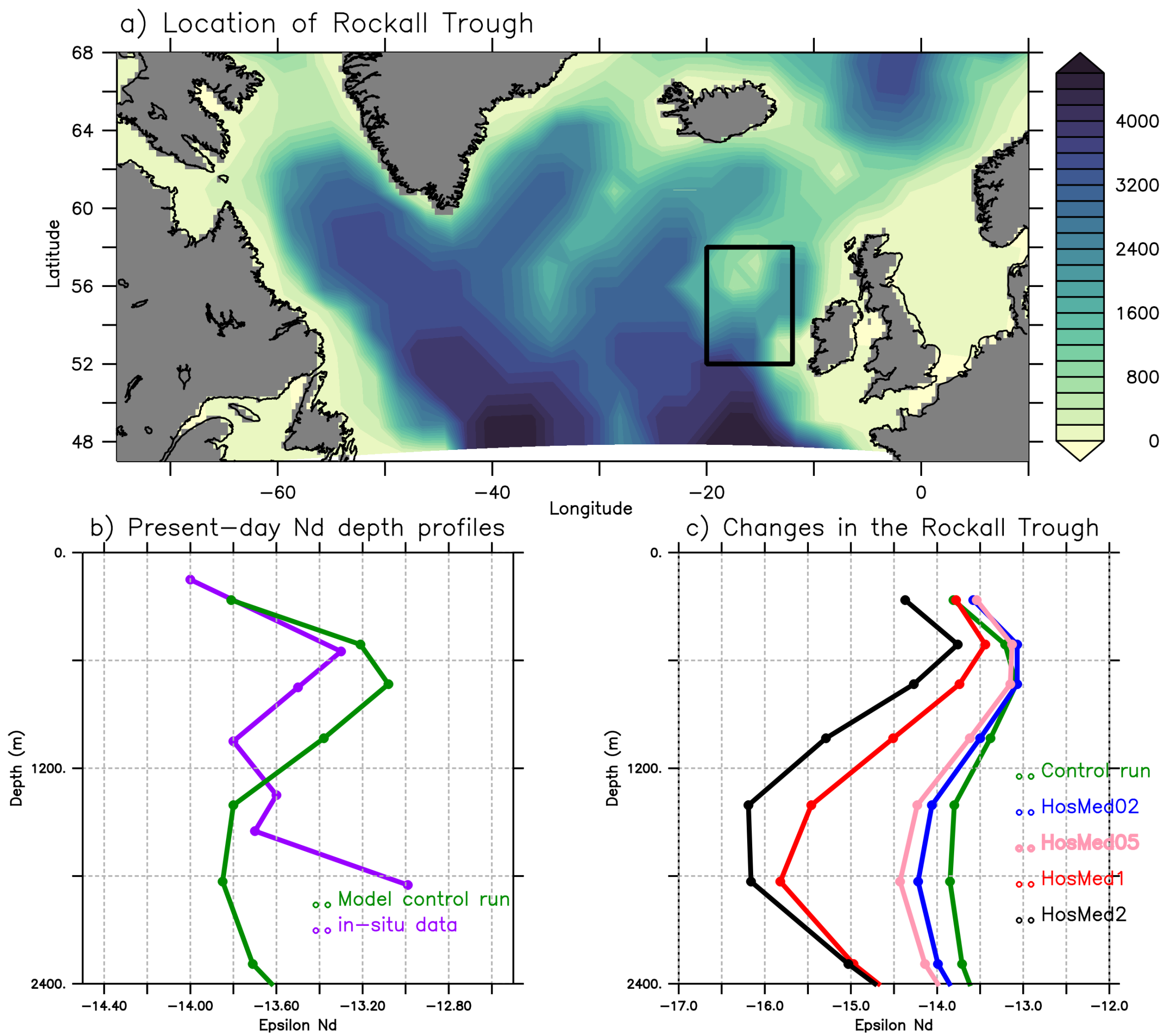

Figure 9. Location of Rockall Trough (grey rectangle in **a**) bathymetry map (in m), **b**) Present day $\varepsilon_{\mathrm{Nd}}$ depth profiles from historical simulation (red line), and from in situ observations (in black) from Dubois-Dauphin et al. (2017). **c**) change in the Rockall Trough from the four Mediterranean hosing simulations.

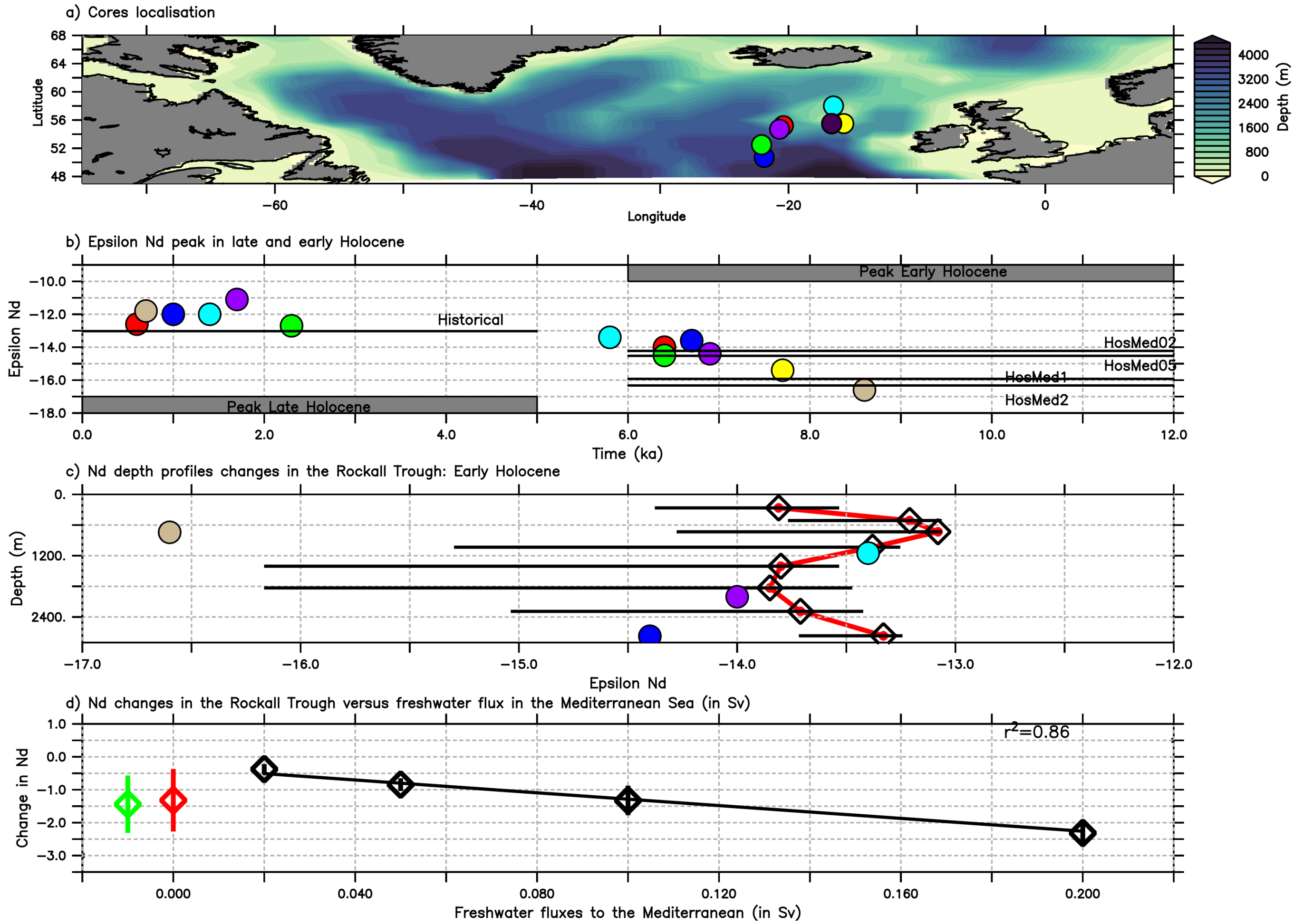

Figure 10. a) Map of the marine sediments cores compiled from Colin et al. (2019); Roberts and Piotrowski (2015), **b**) peak value of ε_{Nd} during the Early and late Holocene from observational records (Color-filled dots) and from model (Shorizontal line), **c**) changes in vertical profile of ε_{Nd} at Rockall Trough during the early Holocene (between 6 and 10 ka): from observational records (Colour-filled dots), and from the model outputs. In red is the control simulation (red line) and the black line corresponds to the range of ε_{Nd} change in the hosing experiments, *i.e* the difference between the control run and the peak value (minimum and maximum) in the four hosing simulations. **d)** changes in the Rockall Trough versus freshwater flux release in the Mediterranean Sea (in Sv). The ε_{Nd} changes in the model (black box) are defined as the difference between the hosing and control experiments at 750m depth averaged over the last 100 years of each simulation. The ε_{Nd} changes from Colin et al. (2010) (red box) and Crocket et al. (2011) (green box) are defined as the difference of the average ε_{Nd} value between the early Holocene (*i.e.* before 6 kyr PB.) and the late Holocene (*i.e.* after 6 kyer BP). The black line corresponds to the curve from a least squares linear regression made with the four hosing simulations (r^2=0.86). The error bars represent the standard deviations computed in the simulations.

Table A1. $\varepsilon_{\mathrm{Nd}}$ anomalies between present-day values from (Tachikawa et al., 2004; Vance et al., 2004; Henry et al., 1994) and $\varepsilon_{\mathrm{Nd}}$ recorded during the Sapropel event in Alboran Sea from (Jiménez-Espejo et al., 2015), Sardinia Chanel from (Dubois-Dauphin et al., 2017), Sicily Strait and Levantine Basin from (Cornuault et al., 2018). The $\varepsilon_{\mathrm{Nd}}$ anomalies from the model simulations are shown in comparison between the control simulation (*i.e* represent the present-day situation) and the four hosing experiments (*i.e* represent the Early Holocene situation).

	Levantine sub-basin	Sicily strait	Sardinia Channel	Alboran sub-basin
Observations	2.7	2.5	-0.73	-0.45
HosMed2	2.7	1.8	-0.9	-0.6
HosMed1	1.5	1.2	-0.6	-0.4
HosMed05	1.2	1.1	-0.3	-0.2
HosMed02	0.01	0.02	0.01	0.03

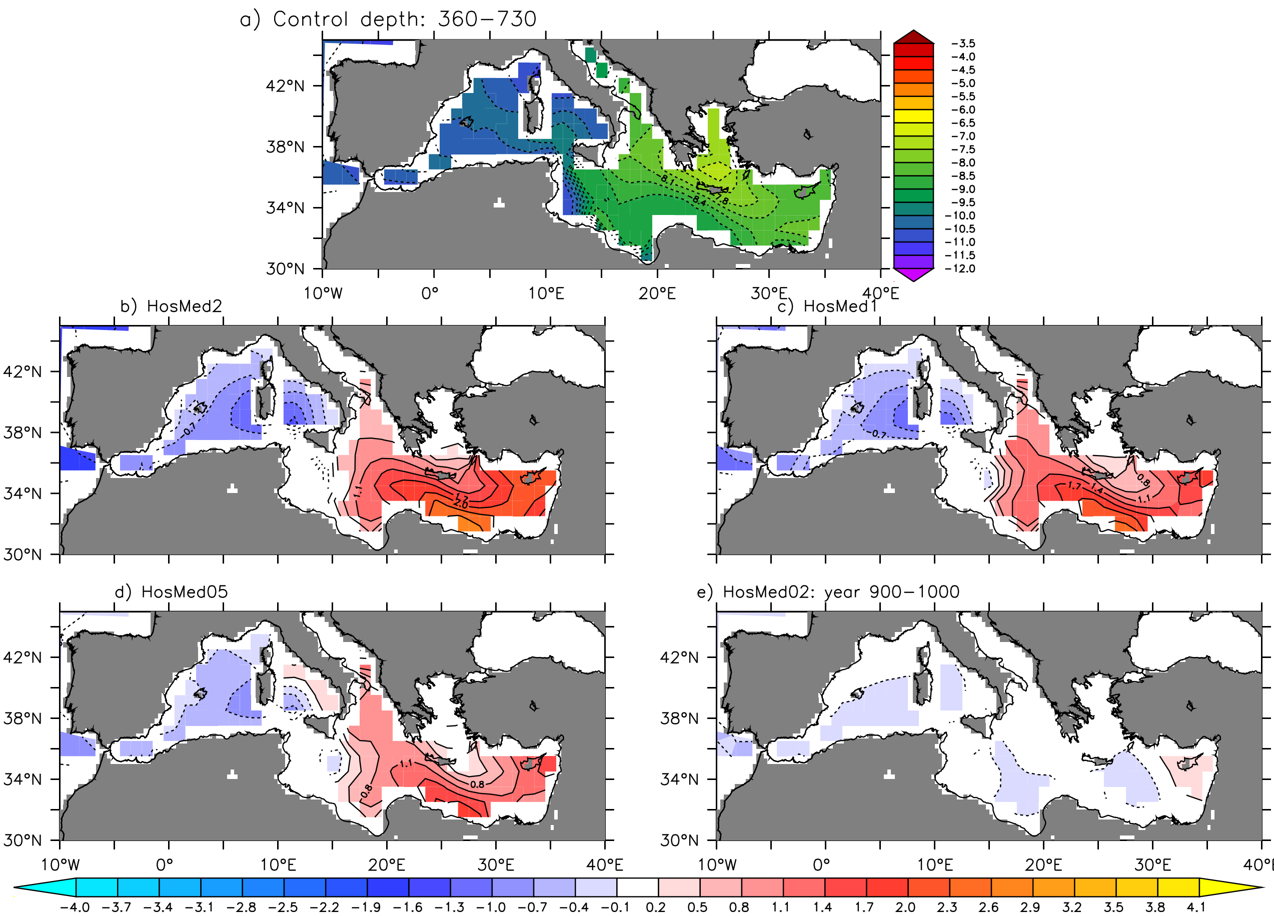

Figure A1. **a)** Horizontal maps of $\varepsilon_{\mathrm{Nd}}$ distribution at 1000 m depth in the Mediterranean Sea. **b)**, **c)**, **d)** and **e)** $\varepsilon_{\mathrm{Nd}}$ anomalies between control simulation and HosMed2, HosMed1, HosMed05 and HosMed02 respectively.

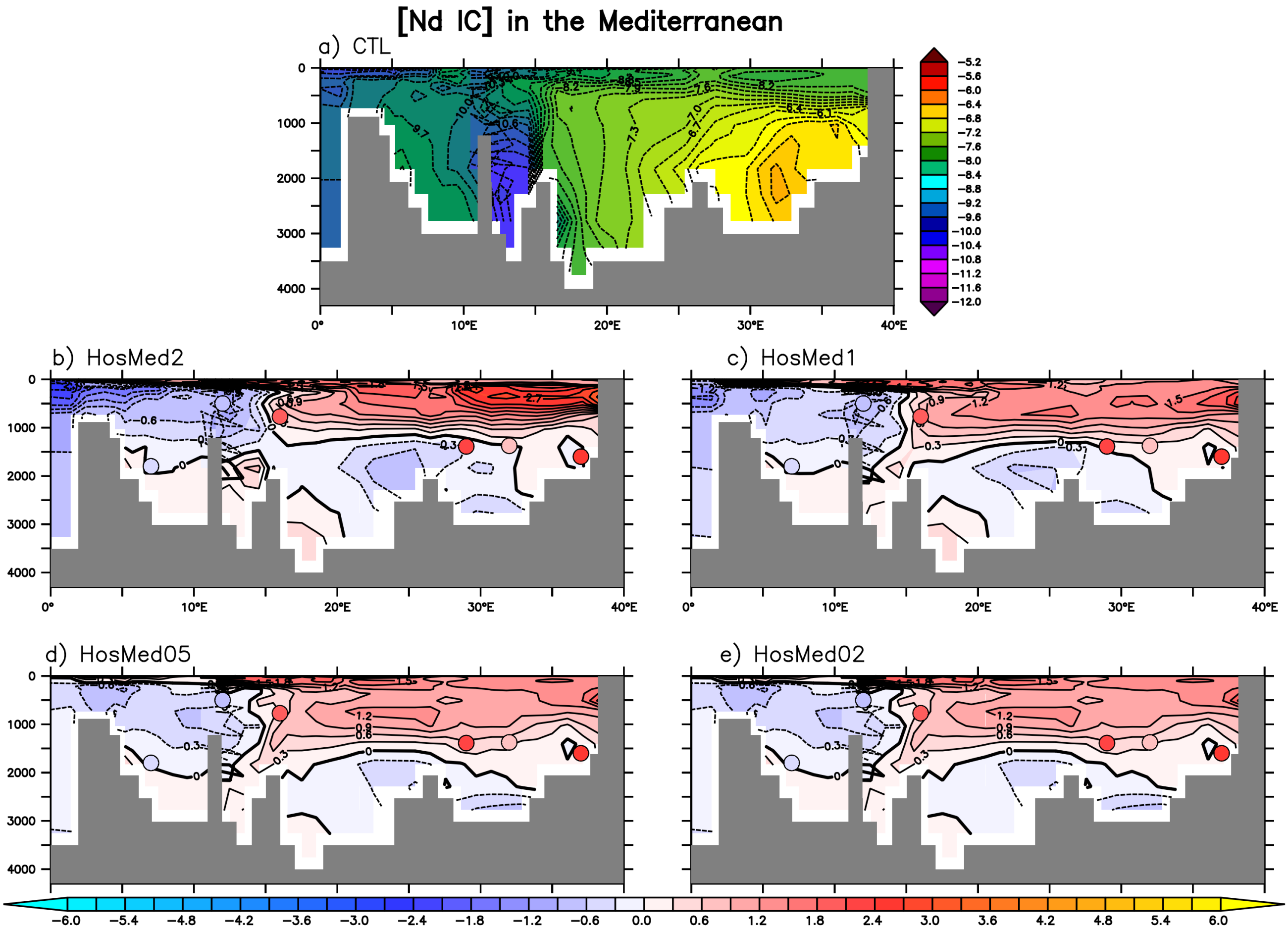

Figure A2. **a)** Vertical sections along an east-west transect in the Mediterranean Sea. **b)**, **c)**, **d)** and **e)** ε_{Nd} anomalies between control simulation and HosMed2, HosMed1, HosMed05 and HosMed02 respectively. Dots represents the ε_{Nd} signal recorded in Alboran Sea (Jiménez-Espejo et al., 2015), Sardinia Chanel (Dubois-Dauphin et al., 2017), Sicily Strait, Levantine Basin (Cornuault et al., 2018), and from Duhamel et al. (2020) for the west-Levantine basin. The data are shown in comparison to modern ε_{Nd} values.

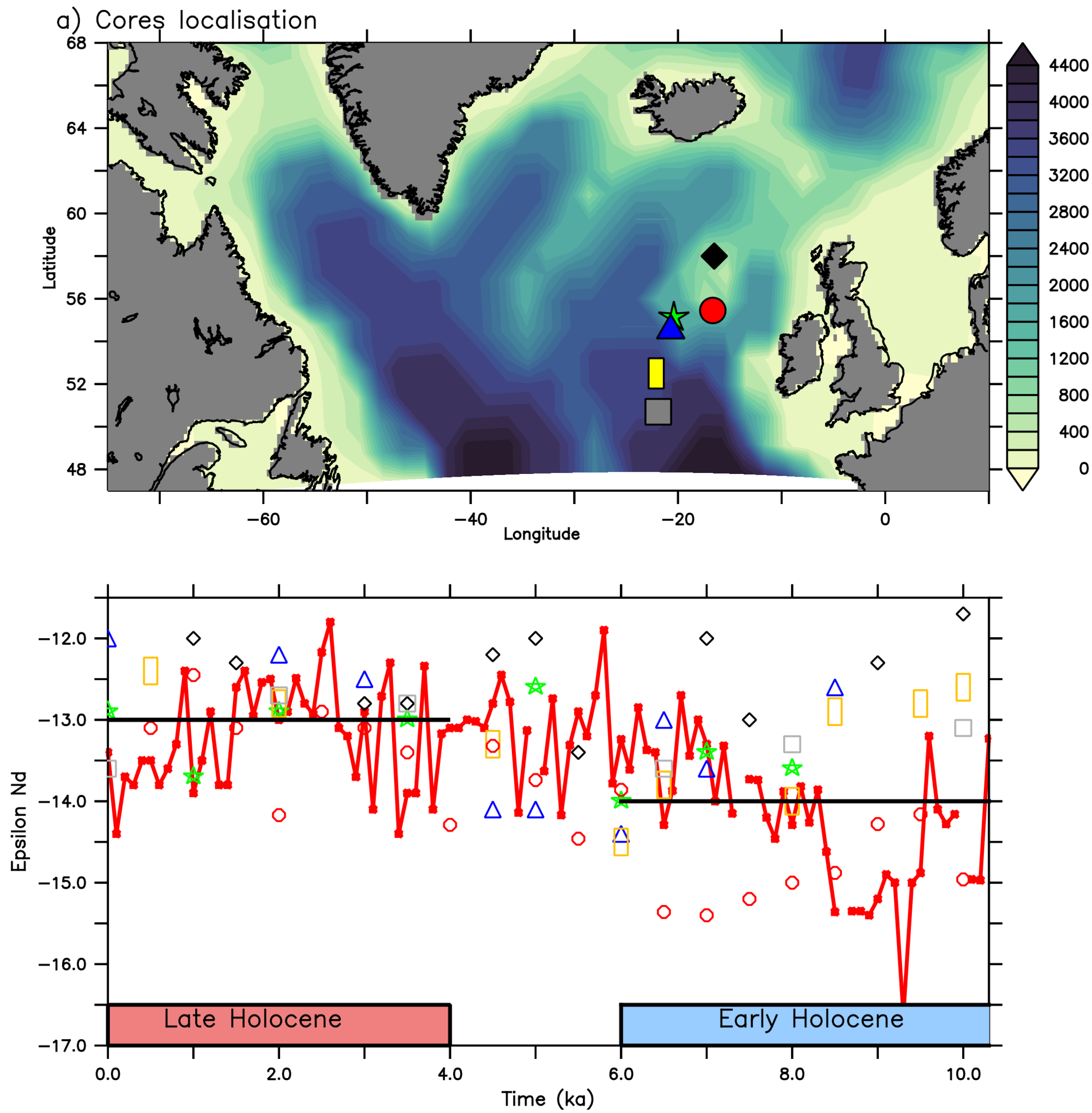

Figure A3. a) Map of the marine sediments cores published in Colin et al. (2019); Roberts and Piotrowski (2015), **b**) Nd isotopic composition (ε_{Nd}) during the Holocene compiled from: Colin et al. (2019); Roberts and Piotrowski (2015). The solid black line represents the ε_{Nd} average value for the Early and Late Holocene as estimated from the same data

Appendix B: Impact of a change in the Mediterranean Sea circulation on the ε_{Nd} distribution

Variations in ε_{Nd} distribution between the control simulation and hosing experiments at 1000 m depth are shown in Fig. A1, as well as vertical sections along east-west transects, which are shown in Fig. A2. The hosing experiments generally reproduces less radiogenic water masses in the western basin, which is a result of reduced exchange with the Eastern Mediterranean basin. ε_{Nd} anomalies are more radiogenic in the Eastern Mediterranean Basin. This is the consequence of the more sluggish circulation simulated in the hosing experiments, which ventilates less deep waters, leading to more stagnant water masses with ε_{Nd} signature closer to the value of the surrounding margins (Fig. A1 and Fig. A2). The maximum of east-west gradient is simulated in HosMed2 (more than 2.5 ε_{Nd} unit of difference), intermediate value simulated in HosMed1 (about 2 ε_{Nd} unit of difference) and HosMed05 (with almost 1.2 ε_{Nd} of difference). On the opposite, HosMed02 keeps qualitatively similar values as in the control experiment (Fig. A1 and Fig. A2).

A few existing ε_{Nd} reconstructions provide data for the last sapropel period in the Eastern Levantine and the Sicily-Tunisian Strait (Cornuault et al., 2018), Sardinia Channel (Dubois-Dauphin et al., 2017), the Alboran Sea (Jiménez-Espejo et al., 2015), the EMed (Wu et al., 2019) and the west-Levantine basin (Duhamel et al., 2020). At the Sardinia Channel, observations display an anomaly in the sapropel order sequence of 0.73 ε_{Nd} (Dubois-Dauphin et al., 2017). It is believed that this situation is the result of a weaker circulation during the Early and Late Holocene. The model is able to simulate less radiogenic values in the water of the Sardinia Channel with a decrease amplitude from -1.8 HosMed2, -0.8 in HosMed1, and -0.6 in HosMed05 (Fig. A2).

The core of the Levantine sub-basin by Cornuault et al. (2018), shows more radiogenic waters during sapropel events than during modern times (+2.7 ε_{Nd}, Fig A2, Table. 1). This can be attributed to the combined effect of a reduced circulation that transports less low-radiogenic water from the western basin, and an enhanced flux of radiogenic materials from the exchange with the margin continent. The model reproduces a similar signal but shallower than in data in HosMed2 (+2.7 ε_{Nd} unit), HosMed1 (+1.5 of ε_{Nd} unit) and, HosMed05 (+1.2 unit). The situation is similar at the Sicily channel (771m) where reconstructions also depict more radiogenic waters during the sapropel compared to the modern seawater signature (+2.5 ε_{Nd}, see Table. A1). The model reproduces the positive signal in HosMed2, HosMed1 and HosMed05. In the core retrieved in the Alboran Sea, an ε_{Nd} signature of -9.75 reported by (Jiménez-Espejo et al., 2015), gives a difference of -0.45 ε_{Nd} with the modern Alboran seawater signature (-9.3, by Tachikawa et al.,2004). The imprint from the hosing experiment reproduces a close signal in HosMed2 (-0.5 ε_{Nd}) and lower signature in HosMed1 and HosMed05. Wu et al. (2019) provide unequivocal evidence for a severe stagnation of waters masses (below $\sim$800 m depth) in the eastern basin consisting with a sluggish between the two basins. The model simulates correctly this disconnection between the eastern and western basin at 1000 m depth in the hosing experiments (cf. Fig. A1) and the fact that HosMed2 exhibits the best fit with observational reconstructions could be related with the approximation of uniform hosing over the whole Mediterranean. Indeed, the freshwater release in the Mediterranean during S1 might have largely occured through increase inflow from river Nile, so that the Levantine basin might have been more impacted than in our idealized hosing experiments.

From this comparison with in situ data, we conclude that IPSL-CM5 hosing experiments lead to similar proportion of $\varepsilon_{\mathrm{Nd}}$ change in the Mediterranean Sea as for the Sapropel event during the mid-Holocene period (cf. Table. A1 and Fig.A1 and Fig. A2).